Fabrication, mechanical properties, and multifunctionalities of particle reinforced foams: a review

Shunze Cao[1,2], Nan Ma[3,4], Yuwu Zhang[5], Renheng Bo[2,*], Yang Lu[6,*]

[1]School of Mechanics and Aerospace Engineering, Southwest Jiaotong University, Chengdu, Sichuan 610031, China

[2]AML, Department of Engineering Mechanics; Center for Flexible Electronics Technology, Tsinghua University, Beijing 100084, P.R. China.

[3]Faculty of Engineering, University of Nottingham, University Park, Nottingham NG7 2RD, United Kingdom

[4]Department of Engineering, Lancaster University, Lancaster, LA1 4YW, United Kingdom

[5]College of Liberal Arts and Science, National University of Defense Technology, Changsha, Hunan 410073, P.R. China.

[6]College of Architecture and Environment, Sichuan University, Chengdu 610065, P.R. China.

Abstract

In the past decade, particle reinforced foams have been intensively studied and applied in diverse fields owing to their low weight-to-strength ratio, low cost, and tailorable physical properties using various matrix materials and additives. In particular, the thin-walled microstructures in foams and certain particles provide excellent energy absorption capacity compared with the solid materials. A considerable number of research findings on particle reinforced foams have been reported from various aspects, including fabrication techniques, matrices and reinforcement types, mechanical responses as well as other physical properties. Up to date, several review articles have been published to partially cover the stated aspects on hollow particles reinforced foams (i.e., syntactic foams). However, discussion on different types of nano/micro-scale solid particles and millimeter-scale porous particles reinforced foams remains insufficient. Therefore, this article aims to provide a comprehensive review on particle (e.g., solid/porous/hollow particles) reinforced foams (made up of metal/polymer/ceramic matrices) covering fabrication techniques, mechanical responses and their multifunctionalities. Particularly, different reinforcing mechanisms and modifications to physical functions of foams with different matrices using various types of particle additives are reviewed. The opportunities for future explorations of particle reinforced foams in the aspects of manufacturing, modeling and applications are discussed lastly.

Keywords: Particle reinforced foams; Reinforcing particles; Foam matrices; Fabrication techniques; Mechanical properties; Multifunctionalities

1. Introduction

Foam materials have advanced rapidly in recent decades due to their broad applications, including packaging, construction, infrastructure, automobiles, aviation, personal protective equipment, and submarines. Neat foam materials are usually constituted by solid thin-walled matrix and hollow cells, where the constitutive materials of thin-walled structures mainly include polymer, metal, and ceramic [1-10]. Metal and ceramic matrices possess high strength/stiffness and temperature resistance; however, their production is rather costly compared to the polymer matrix. Neat foams, manufactured using solid-state method (i.e., the approach applied for open-cell foams, also namely powder metallurgy) or liquid-/gas-state techniques (i.e., the fabrication methods mainly used for closed-cell foams) [10-14], exhibit several advantages such as low density and high energy absorption capacity, while suffered from their low stiffness and strength in real-world applications [2, 15-17]. Therefore, reinforcements such as particles, fibers, carbon nanotubes, and metallic pins have been added to strengthen the foam matrix [18-20]. Particle reinforcements have been studied intensively because of the suitability for large scale production [21, 22]. The dimensions of the reinforcing particles vary from nano to millimeter scale. Solid particles, porous particles, and hollow particles are three common types of particle reinforcements. The hollow spherical particles with thin shells attract more attentions due to their low density-to-strength ratio [23-25]. Foams strengthened using hollow particles (i.e., syntactic foams) exhibit tailorable physical properties and could stabilize the solid matrix structures under various loading conditions. The recent development of particle reinforced foams benefits from the advances of manufacturing techniques, such as highly controllable vacuum-assisted manufacturing systems and additive manufacturing, which allow for rational design to obtain desired physical properties [26-30]. In addition to serving as reinforcements, the particle additions can also modify the thermal, acoustic, and electrical properties of matrix materials, and endow the foams with new property, such as the self-healing [31-38]. Given the above advances, the particle reinforced foams are drawing growing attentions from both academic and industrial communities [39, 40].

In this review, we summarized the recent progress in particle reinforced foams, focusing on the production techniques, mechanical properties, and functionalities. Various morphologies of particle additives and matrix materials are also included. The production techniques and mechanical properties of metal foams, polymer foams, and ceramic foams are presented in Section 2, Section 3, and Section 4, respectively. Section 5 discusses the thermal, acoustic, electrical, and self-healing properties of foams with particle additions. Finally, we provide some perspectives on the challenges and opportunities of particle reinforced foams.

2. Particle reinforced metal foams

Metal foams are a class of porous foam materials fabricated from solid metals (aluminum, aluminum alloy, tantalum, titanium etc.) [41, 42]. At the expense of strength and elastic modulus, neat metal foams are well known for their light weight, high energy absorptions, excellent acoustic insulations etc. [43] compared to the base materials. Such weak strength and low elastic modulus could affect the stability of metal foams during services. To remedy these weaknesses, particle reinforcements have been added to form particle reinforced metal foams.

Fabrication of particle reinforced metal foams

The fabrication methods for neat metal foams include powder metallurgy, stir casting, gas injection, infiltration etc., [44-47]. The fabrication techniques for the particle reinforced metal foams are basically similar to those for neat metal foam. According to the dimensions and morphologies, the particle reinforcements used in metal foams can be divided into two groups, i.e., micrometer-scale solid particles and hollow particles, as shown in **Fig. 1a** and **1b**, respectively [45, 46]. The solid particles are usually located at the solid structs, while the hollow particles are trapped within the cells. The manufacturing strategies are different depending on the morphologies of particle reinforcements.

For instance, the open-cell foams reinforced by micro-scale solid particles are usually manufactured by a solid-state technique [47-49]. Uzun (2019) used the powder metallurgy approach for fabrication of Silicon carbide (SiC) particle reinforced aluminum foams [47]. The manufacturing setup is shown in **Fig. 1c**. In this research, the solid alloy aluminum powder (AlSi12) and SiC particle reinforcements are mixed with blowing agents and compacted within a stainless-steel container. The compacted material is referred to as the precursor which is placed in a mold. The width of compacted material is the same with the internal width of the mold ensure vertical expansion in the foaming process. Then, the mold is placed in a pre-heated furnace. When the heating temperature is above the melting point of the solid metal, the foaming process starts. Although the foams produced via powder metallurgy provide relatively homogenous microstructures, the production process is not widely used due to the high cost and low production. On the other hand, the closed-cell metal foams reinforced by micro-scale particles are usually fabricated using the liquid-state direct foaming technique [50]. For fabrication of aluminum nitride (AIN) particle reinforced aluminum foam, the aluminum powder and AlN particle reinforcements were compacted with melted aluminum alloy under nitrogen environment. The schematic illustration of apparatus used for foaming is shown in **Fig. 1d**. Once the compacted metal composite is heated to reach its melting point, the blowing agent (titanium hydride (TiH_2)) is added into the graphite crucible with constant stir. Gas is generated during the foaming process. Then, the melt is cooled at the room temperature. Besides, to improve the quality of foams produced from the instantaneously foaming strategies of Alcan process (foaming by injecting gas into liquid metals) and Alporas process (foaming by gas-releasing blowing agents), which were developed in 1980s and 1960s, respectively [6, 41, 42], the particles in micro-scale could also be added during the stated processes. In detail, to increase the viscosity and stability of melted metal, the Alcan Hydro process was developed by adding 10%~15% volume fraction of SiC particle reinforcement, as schematically shown in **Fig. 1e**. The internal microstructure was more homogenous after adding particle additives. Besides, the Alporas process is another technique to fabricate aluminum foams. An addition of 1.5% volume fraction calcium was used in

melt for the adjustment of viscosity. Compared to the powder metallurgy, the Alcan and Alporas techniques are more suitable for mass production with requiring simpler tools for manufacturing.

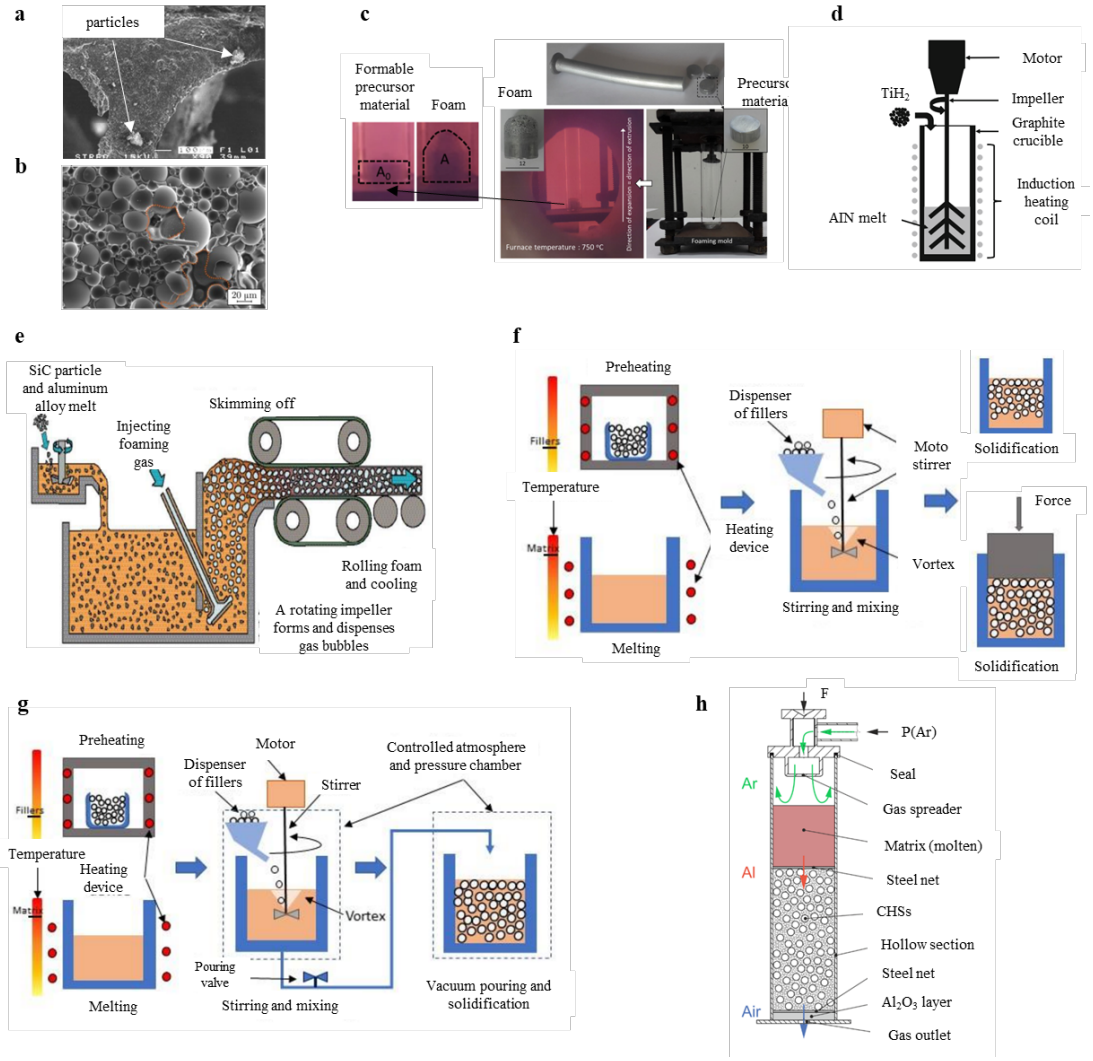

Figure 1 Fabrication techniques of particle reinforced metal foams. (a) SEM image of the cell structure of solid micro-particle reinforced metal foam [45]. (b) SEM image of a cross-section of syntactic metal foam [46]. (c) The precursor material and foaming equipment used in powder metallurgy technique [47]. (d) Schematic illustration of melt foaming process [50]. (e) Schematic illustration of gas injection for the production of particle reinforced metal foams [51]. (f) Schematic drawing of conventional stir casting technique for producing syntactic metal foams [52]. (g) Schematic illustration of vacuum-assisted stir casting technique [52]. (h) Schematic illustration of infiltration technique for manufacturing syntactic metal foams [56].

For the metal foams reinforced by the hollow/porous spherical particles, the producing

techniques of stir casting, powder metallurgy, and low-pressure infiltration can be employed [49, 52-57]. Stir casting is a simple and inexpensive liquid-state technique, where the metal material is heated above the melting point before the stirrer rotates. To fabricate MSFs, the pre-heated hollow particle reinforcements are gradually added into the melted metal matrix. After intense mixing, the composite melt is poured into a pre-prepared mold. The main drawbacks of stir casting technique include the limited volume fraction (VF) of additives and inhomogeneous distribution of particles [52-54]. To increase the VF of fillers, low compressive force could be added onto the top of melted slurries before the solidification, as shown in **Fig. 1f**. The partial buoyancy effect was offset by the external force, which allowed more content of additives. For instance, this modification increased the VF of hollow particles from 30% to 50% within metal foam matrix [52]. To hinder the buoyancy of the fillers, creating a controlled pressure chamber during the solidification (**Fig. 1g**) has been implemented. Compared to the conventional stir casting, the hollow particles can disperse more uniformly by exerting controlled pressure. To produce the MSFs with the desired size of hollow cells and porosity, the low-pressure infiltration technique is used [55, 56], as schematically shown in **Fig. 1h**. The foaming process of low-pressure infiltration technique is relatively complex compared with other methods. The experimental setup of the infiltration process mainly contains a device of gas inlet, a heating furnace, and a chamber for space holder particles. A thick Al_2O_3 quilt layer and a fastened steel net are placed at the mid and bottom of the device to prevent the movement of hollow particles. The device allows for adjustment of the internal gas pressure to ensure the control of infiltration speed. The infiltration device can be used to produce the hollow particle reinforced metal foams with the evenly and homogenously distributed particles of various sized particles. The porosity of reinforced foams can be greater than 65% [55]. The key information of main fabrication techniques for particle reinforced metal foams is listed in **Table 1**.

Table 1. The key information of fabrication technique of particle reinforced metal foams

Technique	Main advantages	Main handicaps
Stir casting	1. Simplicity 2. Low cost	1. Requiring additional conditions for produce foam with good quality
Gas injection	1. Simple and straightforward 2. Mass production	1. Hard to control foaming process 2. Nonuniform cell sizes
Powder metallurgy	1. Homogenous microstructure	1. Improper for mass production 2. The equipment is relatively expensive
Infiltration	1. Homogenous foam microstructure and distribution of particle 2. Suitable for various particle sizes and volume fraction of particles	1. Relatively complicated and expensive

Mechanical properties of particle reinforced metal foams

The morphologies of particles used as the reinforcements in metal foam matrix includes the solid micro-sized particles, porous particles, and hollow particles. The solid micro-sized particles are conducive to increasing the viscosity and stability of metal foams during the manufacturing process, and the mechanical properties of foam can also be enhanced. Up to date, a variety of solid micro-sized particles (e.g., Al_2O_3, SiC, Y_2O_3, TiB_2 etc.) have been used as the stabilizer and reinforcements within the metal foam matrix. However, the reinforcing effects can vary significantly. Li et al. (2007) added various ceramic particles, e.g., B_4C, (cubic boron nitride) CBN, and SiC, into aluminum foams [58]. The peak stress and elastic modulus of neat foams and particle reinforced

foams under quasi-static and dynamic compressions were measured. The experimental results indicated that adding ceramic particles can increase peak stress and elastic modulus, resulting in higher energy absorption capability. Besides, the particle additions led to strain rate sensitivity under dynamic compression. Wichianrat et al. (2012) added varying mass fractions of SiC particles into open-cell aluminum alloy (type AC3A alloy) foams [59]. The SiC particles are embedded in the solid cell walls. The experimental measurements indicate a higher mass fraction of particles resulting in higher energy absorption capability and compressive strength, as shown in **Fig. 2a**. Kulshreshtha et al. (2021) studied the mechanical properties of closed-cell aluminum foams and alloy aluminum foams reinforced by the micro-SiC particles [60]. The quasi-static compressive results indicated that higher plateau stress could be obtained with the increased mass fraction of particles, as shown in **Fig. 2b**. Besides, the alloy aluminum foam presented higher plateau stress and energy absorption capability than neat aluminum foam. From the above findings, the mechanism of improving mechanical properties relates to strengthening cell walls by solid micro-particles. Liu et al. (2009) reported the plateau stress of SiC particle reinforced foams decreased gradually during quasi-static compressions (**Fig. 2c),** which could be induced by the local brittle behavior of the interface between particles and foam matrix [61]. The gradually decreasing trend of plateau stress results in the negative effect of the energy absorption efficiency of particulate foams. From the researches of solid particles reinforced metal foams, the reinforcing behaviors are decided by the micromechanics of interactions between particles and cells.

For the hollow particles, including metal particles, glass particles etc., provide strong support to the surrounding metal foam matrix against loading [56, 62-66]. Szlancsik et al. (2015) studied the aluminum alloy syntactic foams reinforced by hollow iron spheres under compressive loading experimentally and numerically [56]. The experimental observations and finite element calculations captured the collapse mechanism of iron hollow spheres reinforced syntactic foams. During the compression, the hollow spheres were crushed firstly after the yielding, and the matrix followed the deformation of spheres. The left and right sides images in **Fig. 2d** show the internal microstructure of

syntactic metal foams before and after compression, respectively. Broxterman et al. (2020) compared the mechanical properties of glass-aluminum syntactic foams manufactured from stir casting and infiltration casting [62]. The results indicated the foams produced by the stir casting show higher yield strength and plateau stress, due to the close-cell microstructure. In contrast, the foams produced by the infiltration casting exhibited open-cell morphology and the resulting foams had a decreased strength and density. Kannan et al. (2020) compared the compressive responses of neat aluminum alloy foams and thin-walled hollow ceramic particles reinforced aluminum alloy foams [63]. The compressive responses of neat and reinforced foams indicate the evidently higher yield strength with the presence of ceramic hollow cells. The main contributions of particle additives to the mechanical properties of metal foams are listed in **Table 2**.

The porous particles, including expanded perlite, activated carbon particles, expanded glass particles and lightweight expanded clay aggregate particle, show the combined advantages of mechanical enhancement, light weight, and relatively low cost [67,68]. Kemeny et al. (2020) conducted the fatigue tests on zinc aluminum foam embedded with expanded perlite [69]. The results indicated the composite foams provided ideal performances on cyclic compression at various loading conditions. Movahedi et al. (2019) studied the quasi-static compressive responses of activated carbon particle reinforced magnesium foam with low density (1.12–1.18 g/cm−3), where higher density contributed to higher compressive stress-strain curves [70]. Aside from the uniform metal foam matrix, the mechanical properties of graded metal composite foams reinforced by porous particles have also attracted research interests in recent years owing to the advantages of tunable properties. For instance, Movahedi et al. (2019) developed a novel functionally graded metal foam reinforced by porous activated carbon particles and porous expanded perlite with two separated layers. The quasi-static compressive test results indicated that better energy capacity could be achieved compared to the particle reinforced foams with single layer [71]. Su et al. (2019) developed the hybrid particles reinforced metal foams containing porous expanded glass particles and alumina hollow spheres [72]. It is shown that the stress-strain curve of hybrid reinforced syntactic foams was higher than that of expanded glass particles

reinforced foams, but lower than that of hollow particle reinforced foams.

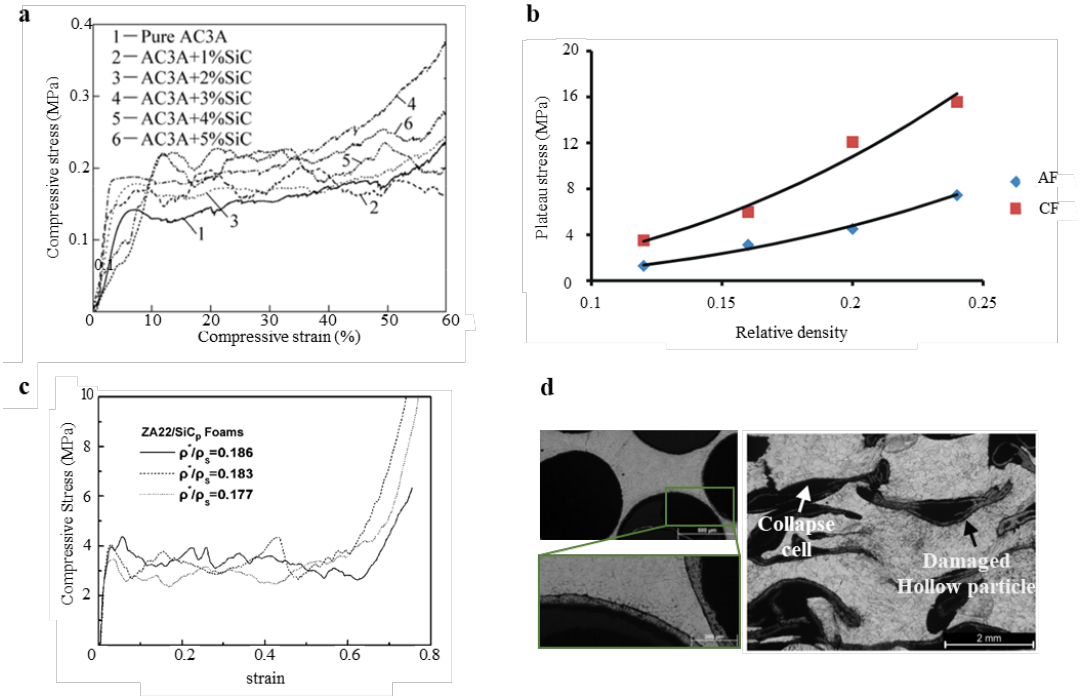

Figure 2 Mechanical responses of particle reinforced metal foams. (a) Quasi-static compressive responses of open-cell aluminum alloy (type AC3A alloy) foam and SiC particle reinforced type AC3A aluminum alloy foams [59]. (b) The plateau stress obtained from particle reinforced aluminum foams with various particle contents as a function of relative density of foams [60], where AF represents aluminum foams and CF represents SiC particles reinforced composite foams (c) Compressive responses SiC_p particle reinforced Zn-22Al aluminum alloy foams with various relative densities [61]. (d) The optical images of cross-section of glass/aluminum syntactic foam before loading (left images) and after compression (right image) [62].

With the presence of particle additives, the reinforced metal foams still yield the triphasic phases of compressive behaviors (i.e., elastic phase, plateau phase, and densification phase). Besides, the reinforcing mechanisms of particles in micro and millimeter scales are different. The solid particles in microscale increase the density of solid cell structs, while the hollow and porous particles in millimeter scale stabilize the cells during deformation.

Table 2. The reinforcing behaviors and mechanisms of solid particles and hollow particles to the metal foam matrix.

Types of particle additives	Main contributions to mechanical responses	Mechanisms
Solid micro-sized particles	1. Stabilize the foam microstructure	1. Increase the viscosity during foaming process
	2. Increase the mechanical properties and energy absorption capability	2. Cell walls are strengthened by particles
	3. Decrease of plateau stress due to particle cracks	3. Local damage between particles and foam matrix
Hollow particles	1. Increase the mechanical properties and energy absorption capability	1. Stabilize the cell and provide support to the surrounding metal foam matrix against loading

3. Particle reinforced polymer foams

Polymer foams, comprised of polymer matrix and hollow cells, have been applied for numerous industrial and household applications. The polymer foams can be classified into thermoset and thermoplastic foams [73,74]. The thermoset polymer cannot be melted, and the solidification process is irreversible. In contrast, the thermoplastic polymer can be melted and reformed. When comparing with solid polymers, except for the advantage of lightweight, the polymer foams also show good thermal/electric insulation benefiting from the porous nature. However, their high porosity leads to the loss of mechanical properties. Therefore, to further enhance the mechanical properties of neat polymer foams, either porous or hollow particles have been added to the foam matrix.

Fabrication of particle reinforced polymer foams

A commonly used technique for producing particle reinforced thermoset foams is stir casting [75-78]. For the thermoset epoxy foam foaming in room temperature, the

particles are dispersed in the liquid epoxy resin directly [75], as shown in **Fig. 3a**. Then, the hardener is added to trigger the foaming process. After curing, the hollow glass microspheres (HGMs) are trapped within the foam matrix. During the mixing, the problems of pre-curing and the damage of particles may occur. Besides, due to the differences in density between liquid and particles, the distribution of particles could be inhomogeneous [79,80]. To solve the inhomogeneous distribution problem, external pressure should be exerted. Wu et al. (2016) and Jiang et al. (2020) used the vacuum-assisted stir casting. For instance, the mixed solutions and particles are heated in a vacuum drying oven to decrease the buoyancy effect, as shown in **Fig. 3b**. After curing, the particle reinforcements were reasonably distributed within the polymeric foam matrix. Moreover, Yu et al. (2018) developed a vacuum-assisted resin transfer mold (VARTM) strategy to avoid the buoyancy effect more effectively [81], as shown in **Fig. 3c**. The expanded polystyrene beads/hollow glass microspheres reinforced epoxy foams were produced from the experimental setup. In the first step, an impeller mixed the hollow glass particles with resin and hardener, while the expanded polystyrene beads were filled into a mold. Then, the mixed resin composite was poured into a container upon a vibrator to ensure the glass particles dispersed evenly. After well mixed, the vacuum pump was turned on to start the injection process. The compressed air generated by the vacuum pump pulled the resin composite flowing into the mold, which contained expanded polystyrene beads. whereafter the fabrication process, both solid polystyrene beads and hollow glass beads were distributed homogeneously within foam matrix. For the production of thermoplastic foams, the heating process is essential. The injection molding technique is often used to produce thermoplastic particle reinforced foams [40,76,82-87]. Qi et al. (2020) fabricated the particle reinforced thermoplastic foams [76]. In the first step, the hollow glass particles with 50% volume content were thoroughly mixed with the resin system. Then, the mixture was poured into a hooper, which was placed on an extruder, as shown in **Fig. 3d**. Then, the heating process was activated, and the extrudate was granulated to an injection molding machine. The gas was delivered into the mold to trigger the foam process. Apart from mold injection, the particle reinforced thermoplastic foams can also be produced by mold casting technique

[88,89], as schematically shown in **Fig. 3e**. In this method, the chemical blowing agent should be mixed with the polymer and reinforcements. Then, the mixed composites are transferred to the mold. The chemical blowing agent is decomposed to gas, such as N_2, CO_2, during heating to trigger the foaming process. Besides, the technique of compression mold has also been adopted, allowing the production of large-scale thermoplastic particle reinforced foams [90-92]. For instance, Jayavardhan et al. (2017) developed glass microballons reinforced thermoplastic foams by compression mold. The molding process was optimized in screw rotation speed avoiding the particles fracture. The flexural modulus of hollow particle reinforced foams increased while the strength decreases with increasing filler content, and the tensile strength of those decreased with rising filler content [90]. In recent years, the additive manufacturing technique has been employed to fabricate particle reinforced polymer foams [26,94-97]. Nawafleh et al. (2020) developed a vibration-assisted direct-write 3D printing setup to produce particle reinforced thermoset foams [96]. The 3D printer is schematically shown in **Fig. 3f**. Briefly, the well-mixed epoxy resin and particles were poured into a barrel container. Then, a motor-driven piston was used to inject the mixed resin into an extruder. The extruder pushed the mixed resin flowing to the printing nozzle when the printing process started. The internal structure of printed particle reinforced foam is shown in **Fig. 3g**. The 3D printing method provides the potential for the in-situ manufacturing of particle reinforced foams with desired geometry and mechanical properties, although the polymer library is till limited up to date. The key information of main fabrication techniques for particle reinforced metal foams is listed in **Table 3**.

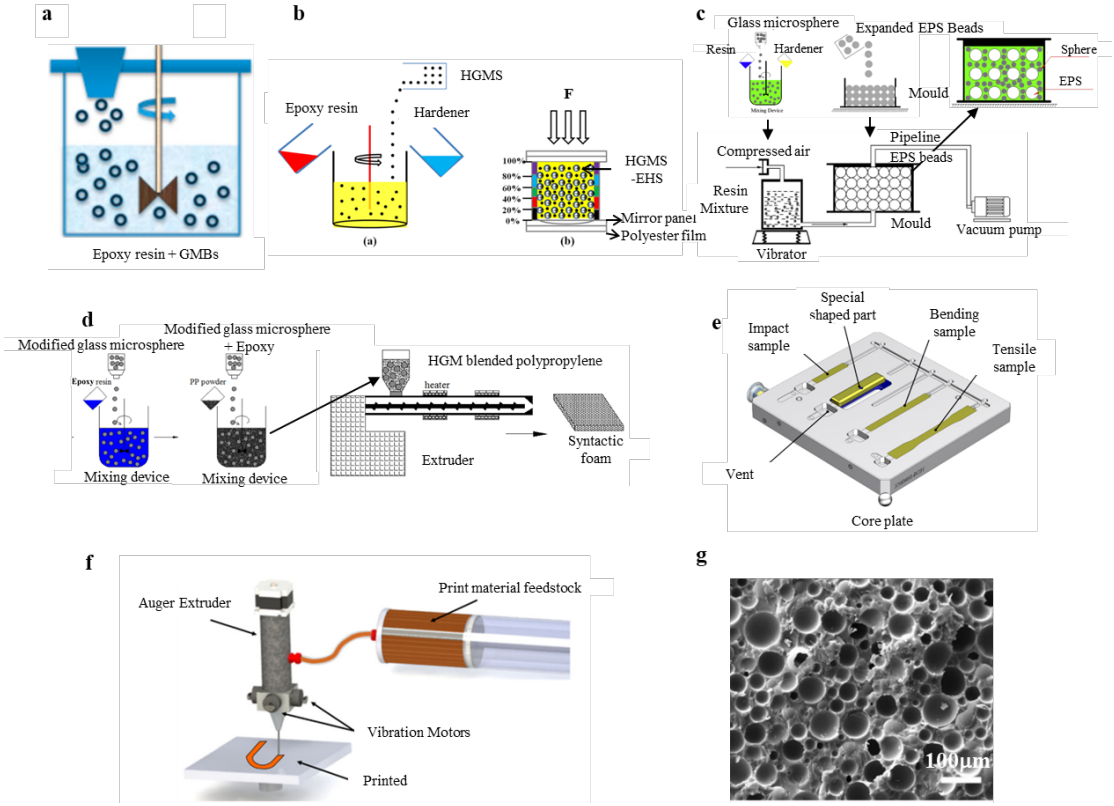

Figure 3 Fabrication techniques of particle reinforced polymer foams. (a) Schematic illustration of direct stir method for fabricating glass microbeads (GMBs) reinforced polymer foams [75]. (b) Schematic illustration of the producing process of HGMs and epoxy hollow spheres (EHs) reinforced epoxy foams via exerting pressure [79]. (c) Schematic illustration of fabricating process of epoxy syntactic foam via the VARTM technique [81]. (d) Fabrication process of polypropylene (PP) syntactic foams via injection method [76]. (e) Schematic illustration of a mold used for producing particle reinforced foams [88]. (f) Experimental setup of a 3D printing system for producing particle reinforced polymer foams [96]. (g) Cross-section a syntactic polymer foam fabricated via 3D printing [96].

Table 3. The key information of fabrication technique of particle reinforced polymer foams

Technique	Main advantages	Main handicaps
Casting	1. Simplicity 2. Low cost 3. Mass production	1. The distribution of particles could be inhomogeneous 2. Premature solidifications 3. Cracks of fillers during mixing
Vacuum assisted	1. Homogenous	1. Relatively high requirement

injection casting	foam structure 2. Suitable for high volume fraction of particles 3. Suitable for multi-scale of particles	for tools 2. Long instrument set-up time
Additive manufacturing	1. Homogenous foam structure 2. Tailorable mechanical properties 3. Complex geometries 4. In-situ production	1. Small-scale production 2. Limitations of material library

Mechanical properties of particle reinforced polymer foams

Polymer foams have been widely used as the structural components of sandwich panels in the applications of packages, buildings, infrastructures, ships etc. A variety types of particles (solid particles, porous particles, and hollow particles) and sizes of particles (from micrometer to millimeter) have been employed as reinforcements for the improvement of strength, stiffness, and energy absorption purposes.

The constitutive materials used for solid particle reinforcements include metal [98,99], rubber [100,101], [102-104], etc. Sorrentino et al. (2010) studied the compressive behaviors of iron particle (lower than 44 μm diameter) reinforced polyurethane foams. With the intervention of magnetic field, the iron particles showed the anisotropic behaviors. When the magnetic field was horizontal to the compressive direction, the reinforcing effect is more pronounced than in the vertical direction. The magnetic force exerted upon the iron particles show the strong support to resist the compressive deformation [98]. Huang et al. (2020) studied the quasi-static and dynamic compressive responses of ceramic particle (0.5mm diameter) reinforced polyurethane foams [102]. The results indicated that the strength and plateau stress of foams are enhanced by the ceramic particles. The strain sensitivity analysis showed that the compressive responses were influenced by the particle cluster effect and stress wave dissipation.

For the porous particle additives in millimeter scale, the mechanical enhancement is

captured by the cell's stabilization and the increase of energy absorption is conducive to the gradual collapse of porous particles during deformation. Cao et al. (2019) studied the quasi-static compressive responses of porous ceramic particle reinforced linear low-density polyethylene foams [2]. The experimental measurements revealed that the reinforcing effects enhanced the elastic modulus, yield strength, plateau stress. Besides, the analyses of energy absorption indicated that the presence of porous ceramic particles provides higher energy absorption capacity per unit volume at a given maximum permitted stress, which can be used in package application, as shown in **Fig. 4a**. Then, Cao et al. (2021) developed a finite element (FE) modelling strategy to study the deformation and reinforcing mechanisms of porous glass beads reinforced polymer foams under quasi-static compressions [2]. The cells and particles were both modelled explicitly in the FE simulations, as schematically shown in **Fig. 4b**. The reinforcing mechanism was explained by the reinforcing effects of glass particles in the undeformed region. **Fig. 4c** presents the stress analysis of particles. The damage is initiated at 25% strain, and at the onset of densification (50% strain), some particles are completed crushed. Brown et al. (2011) investigated the dynamic compressive responses of porous glass beads reinforced polymer foams [105]. The internal microstructure of reinforced foam is shown in **Fig. 4d**. A split Hopkinson pressure bar was used to exert the compressions with various strain rates. The experimental and numerical results indicate that with the increase of the content of glass particles, the yield stress and plastic flow stress are increased, as shown in the left plot in **Fig. 4d**. Meanwhile, the shock wave velocity decreases with the increase of volume fraction of particles. The abbreviation LP shown in the plot represents the volume fraction of glass particles. Cao et al. (2022) employed the Kolsky bar system to study the dynamic compressive responses of porous glass particles reinforced foams with various volume fractions of particles [106]. The Kolsky bar system is schematically shown in **Fig. 4e**, where the cylindrical projectile was accelerated by a gas gun and the stress history in foams was calculated based on the strain gauge signal amplified by an amplifier system. The experimental and numerical measurements of compressive responses under different loading rates are plotted in **Fig. 4f**. It is reported that higher strain rates

contribute to enhancements of elastic properties and plastic stress of GBs reinforced foams with lower and higher particle volume fractions, respectively. It can be concluded from these studies; the porous particles efficiently increased the energy absorption capability and dissipate the kinetic energy. The kinetic energy is dissipated and turned into the internal energy with the gradual collapse of porous particles during deformation. The hollow particle reinforced foam is also referred to as syntactic polymer foams [95,107-109]. Kumar et al. (2016) investigated the quasi-static and high strain-rate compressive response of glass hollow particle reinforced high-density polyethylene (HDPE) foams [107]. The internal structure of particle reinforced foams is shown as the left SEM image in **Fig. 4g**. The experimental measurements reveal that the yield strength increases with the rise of strain rate. The addition of hollow particles increased the yield strength of foams at a low strain rate. However, the reinforcing effect is not pronounced in the scenario of high rates, as shown in the right plot in **Fig. 4g**. The number shown in the plot represents the volume fraction of added hollow particles. Except for the compressive behaviors, the tensile responses of hollow particle reinforced foams were also investigated. Yousaf et al. (2022) studied the tensile responses of hollow particles reinforced polymer foams [108]. The results reveal that a higher volume fraction of particles increases the stiffness of the polymer matrix. However, embedded particles exhibit lower breaking strains than the neat polymer foam due to the debonding of the interface between foam matrix and particles, as shown in **Fig. 4f**. From the above reviews, the particle additions mainly contribute to the enhancement of yield strength and Young's modulus in elastic region, although the stress-strain cures could present the local fluctuation due to the damage of particles. The main contributions of particle additives to the mechanical properties of polymer foams are listed in **Table 4**.

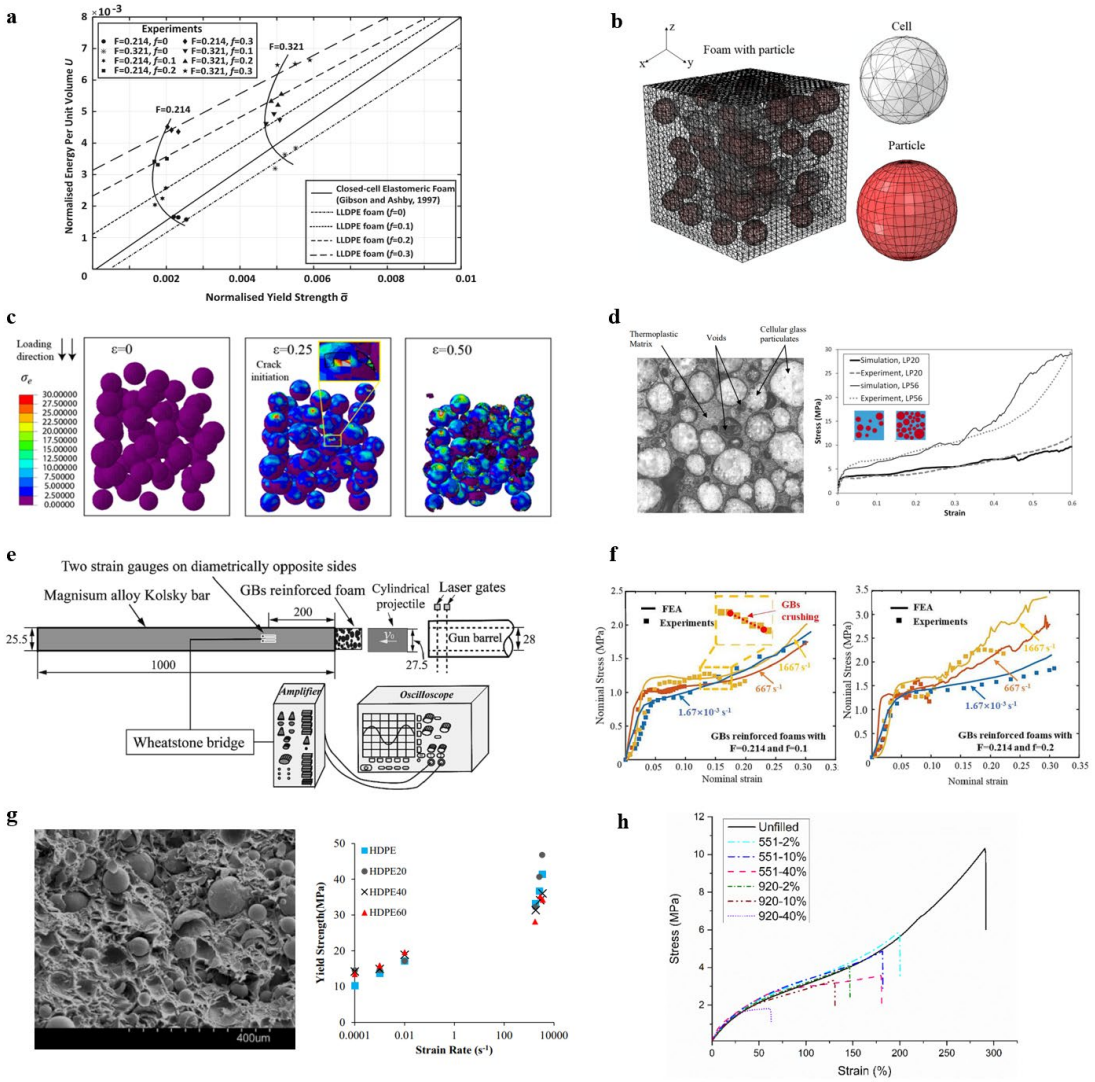

Figure 4 Mechanical responses of particle reinforced polymer foams. (a) Compressive stress-strain responses of neat and porous particle reinforced polymer foams in the left plots, and energy absorption capability per unit volume, as a function of the normalized yield strength of porous particle reinforced polymer foam shown in right. The alphabets F and *f* represent the volume fraction of solid polymer and volume fraction of ceramic particles, respectively [2]. (b) Mesh strategy of 3D FE model of particle reinforced foams [2]. (c) Stress contour of particles under quasi-static compressions obtained by FE simulations [2]. (d) Optical image of internal microstructure of porous glass particle reinforced thermoplastic foam (left image) and compressive responses of particle reinforced foams with various particle contents (right plot) [105]. (e) Schematic illustration of Kolsky system for measuring dynamic compressions of porous glass particles reinforced foams [106]. (f) Numerical and experimental compressive responses of porous glass particles reinforced foams with various volume fraction of polymer (F), particles (f), and loading rates [106]. (g) SEM image of the cross-section of HDPE syntactic foam (left) and yield strength of particle reinforced foams with various particle contents under several loading rates [107]. (h) Cyclic tensile responses of syntactic thermoplastic foam with various particle contents (left plots) and

monotonic tensile responses of neat and syntactic foams [108].

Table 4. The reinforcing behaviors and mechanisms of solid particles, porous particles, and hollow particles to the polymer foam matrix.

Types of particle additives	Main contributions to mechanical responses	Mechanisms
Solid particles	1. Increase the mechanical properties and energy absorption capability 2. Tailorable mechanical properties	1. Particle cluster effect and stress wave dissipation 2. The presence of additional physical field
Porous particles	1. Increase the mechanical properties and energy absorption capability	1. Reinforcing effects in the undeformed region 2. Kinetic energy is dissipated with the gradual collapse of porous particles
Hollow particles	1. Increase the mechanical properties and energy absorption capability 2. More brittle in tension	1. The debonding of the interface between foam matrix and particles

4. Particle reinforced ceramic foams

The development of ceramic foams could retrospect to the 1970s when aluminum oxide and clay were reported [110]. After several decades, ceramic foams have been applied for many high-performance applications, e.g., aerospace, electronic field, medical materials etc., owing to their low density, high strength, uniform cell size, and great stability. Many types of ceramics such as clay, silicon carbide, zirconia, and carbon have been used as ceramic foam matrix materials [111-114], and the usage of particle additives includes the component of cell structs and reinforcements.

Fabrication of particle reinforced ceramic foams

Various techniques have been used to produce particle reinforced ceramic foams, including direct foaming, gel casting, stir casting, sacrificial template technique, reinfiltration, and replica method etc. [114-124]. For the component of cell wall structs, Sarkar et al. (2015) used surface-modified Al_2O_3 particles and carbon fiber to fabricate particle reinforced ceramic foams using direct foaming strategy, as shown in **Fig. 5a** [115]. The first step is the mixing of surface-modified Al_2O_3 suspensions and fibers. After thoroughly mixing, air bubbles were trapped by the mixture of a liquid agent, ceramic particles, and fibers. Then, the wet composite was sintered and dried in a furnace to form the particle-fiber reinforced ceramic foam. The reinforced ceramic foams always present high porosity produced by direct foaming strategy. The microstructure of foams is shown in **Fig. 5b**. Yu et al. (2011) also employed direct foaming technique to fabricate the Al_2O_3/Y_2O_3 particle reinforced Si_3N_4 ceramic foams [118], as shown in **Fig. 5c**. where the Si_3N_4 particles form the cell structs. Zhang et al. (2019) used complex sacrificial template method to produce the alumina particles reinforced ceramic foams [119], as shown in **Fig. 5c**. Firstly, the alumina slurries were degassed and thoroughly mixed with the solvent of catalyst, initiator etc. Then, the mixed agent was poured into the mold, which was fully packed with polystyrene spheres. After the polymer had cross-linked and the slurry had solidified under ambient conditions, the samples were carefully removed from the mold and then dried. Finally, the dried samples were degassed and sintered in a furnace. The particles form the cell walls shown in **Fig. 5d**. The geometry of microstructure of foam is customizable based on the template. For the purpose of reinforcements, hollow particles have been applied. Ozcivici and Singh (2005) proposed a technique combining repeated infiltration and pyrolysis to manufacture ceramic foams reinforced by hollow particles [120], as schematically drawn in **Fig. 5e**. In the first step, the hollow particles were mixed and compacted with the polymer precursor in a liquid state before being placed in a coated mold by the release agent. Then, the pyrolysis process was carried out in a furnace with a continuous nitrogen flow to avoid material oxidation. During the pyrolysis, the porosity of foam would be affected due to the loss of hydrogen from polymer molecules.

Then, the reinfiltration process was implemented to control the porosity of composite foam several times. The cross-sections of particle reinforced ceramic foams are shown in **Fig. 5f**. The hollow particles are located more uniformly with the increase of reinfiltration times. For the replica technique, synthetic or natural template are used as the impregnation of a cellular structure. Then, the template is coated with a ceramic slurry. When the slurry is dried, the template is burned out, and the ceramic particle reinforced foam remains. The microstructure of foams can be controlled by replica technique, but, the mechanical properties are weak due to the intrinsic defects during fabrication [123,124]. The key information of main fabrication techniques for particle reinforced ceramic foams is listed in **Table 5**.

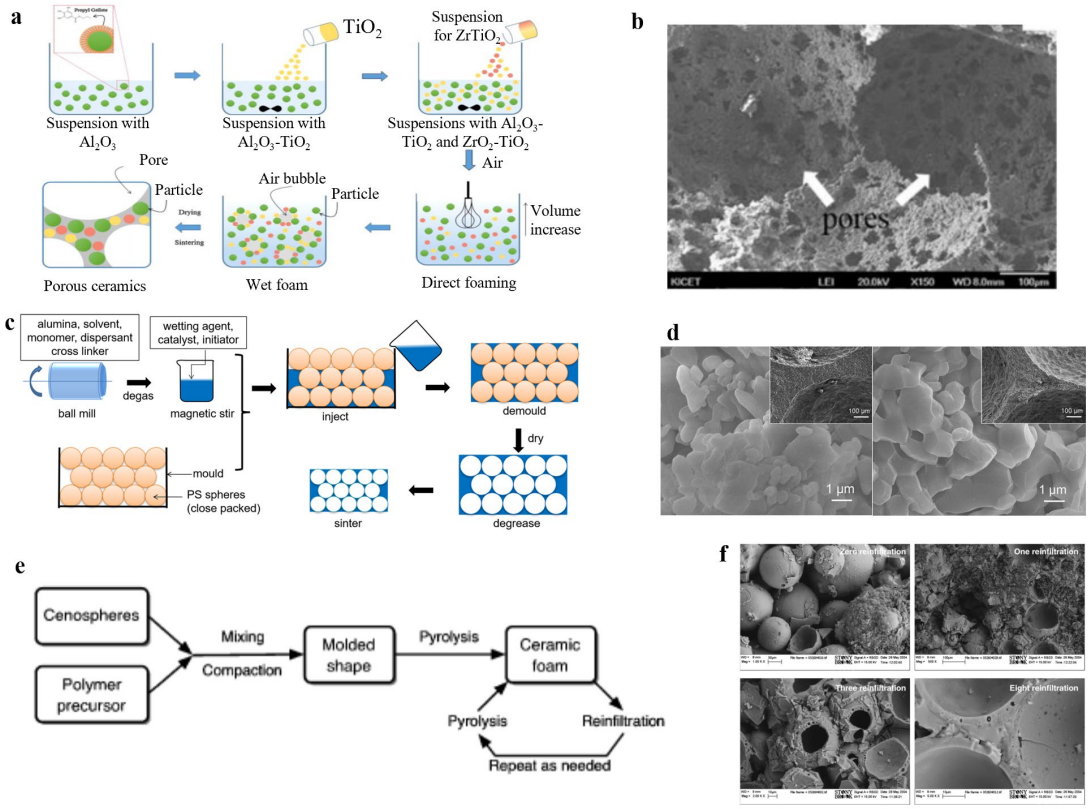

Figure 5 Fabrication techniques of particle reinforced ceramic foams. (a) Fabricating process of direct foaming technique [115]. (b) Manufacturing process of the combination of repeated infiltration and pyrolysis for producing particle reinforced ceramic foams [115]. (c) SEM images of cross-sections of alumina particles reinforced ceramic foams at a variety level of reinfiltration [119]. (d) The SEM image of internal microstructure of particle reinforced Si_3N_4 ceramic foams (right image) and the detailed distribution of particles (left image) [119]. (e Fabrication process of ceramic particulate foams with the combination of gel casting and sacrificial templates [120]. (f SEM image of particles locating at cell walls [120].

Table 5. The key information of fabrication technique of particle reinforced metal foams

Technique	Main advantages	Main handicaps
Direct foaming	1. High porosity 2. Simplicity	1. Premature solidifications 2. Damage of fillers during mixing
Reinfiltration	1. Controllable of microstructure 2. High porosity	1. Long time fabrication 2. High production cost
Sacrificial template	1. Customization 2. Highly porous with uniform pore size	1. Complex fabricating process
Replica	1. Graded or layered microstructure	1. The presence of residual cracks

Mechanical properties of particle reinforced ceramic foams

Except for acting as the constitutive materials of solid cell structure within foam matrix, the micro-scale ceramic particles have also been used as the reinforcements [117, 125-127]. Zhang (2004) added Al_2O_3/Y_2O_3 particles into silicon carbide (Si_3N_4) ceramic foam matrix [125]. The microstructures of cell walls with and without particles are shown as the left and right SEM images in **Fig. 6a**, respectively. With the interventions of Al_2O_3/Y_2O_3 particle reinforcements, the cell walls are stabilized, and the fracture strength increases apparently, as shown in **Fig. 6b**. Pokhrel et al. (2011) and Pokhrel et al. (2013) investigated the reinforcing effect of colloidal amphiphilic particles reinforced ceramic foams [117,126]. The presence of amphiphilic particles increased the density of sintered ceramic foams with less air content due to the in-situ hydrophobization. The microstructure of colloidal amphiphilic particles reinforced ceramic foams are shown in **Fig. 6c** (optical image at left and SEM image at right). With the increased content of amphiphilic particles, the reinforced ceramic foams present higher compressive strength, as shown in **Fig. 6d**. Huo et al. (2019) studied compressive responses of the zirconia/alumina particulate ceramic foams fabricated by

various methods [128]. The SEM image shown in **Fig. 6e** illustrates the reasonable distribution of zirconia (the white grains) and alumina (the dark grains) particles at a cell wall. The experimental measurements indicated that the composite ceramic foams possessed high porosity (above 96%) and excellent specific strength due to the synergistic stabilization of zirconia and alumina particles. The plot presented in **Fig. 6f** summarizes the compressive strength of ceramic foams produced by various methods. The zirconia/alumina particulate ceramic foams presented a relatively high compressive strength compared to others at a low-density range. Then, Liu et al. (2020) developed the Al_2O_3-Si-boehmite particulate ceramic foams [127]. The compressive responses of neat Al_2O_3 ceramic foam, Si particle reinforced Al_2O_3 foam, and Si-boehmite particle reinforced Al_2O_3 foam were measured. From the experimental measurements, the Si additions increased the compressive strength compared to the neat foams. Furthermore, with the intervention of boehmite sol, the foam matrix became more stable due to the enhancement of chemical bonds between Al_2O_3 and Si particles within cell walls. The comparison of composite ceramic foams with various mass ratio of compositions are shown in **Fig. 6g**. The detail compositions of each ceramic foam are listed in **Table 6**. From the above review, the additional nano/micro particles could stabilize the ceramic cell structs, resulting the enhancement of macro-mechanical responses of ceramic foams.

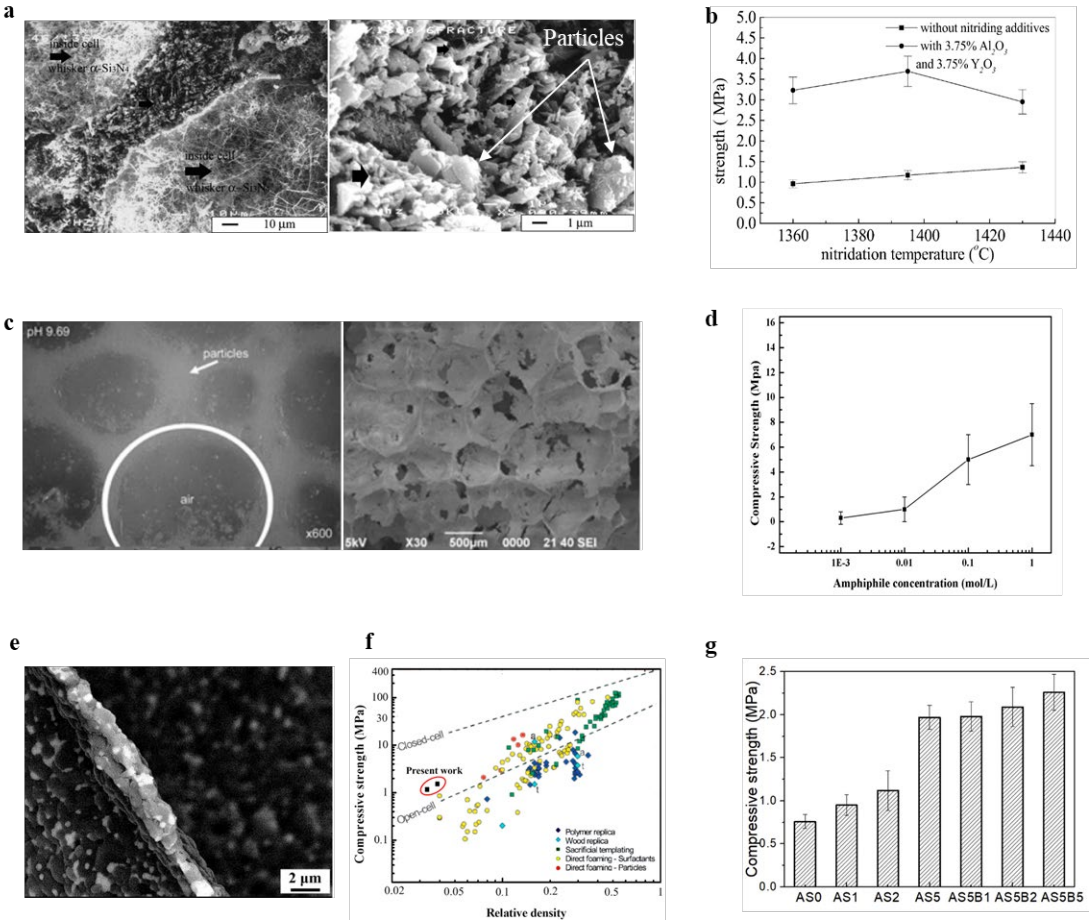

Figure 6 Mechanical responses of particle reinforced ceramic foams. (a) SEM images of neat ceramic foam (right) and Al_2O_3/Y_2O_3 particle reinforced ceramic foams [125]. (b) The relations between fracture strength and nitridation temperature of neat and particle reinforced ceramic foams [125]. (c) Internal microstructure of ceramic particle reinforced foams observed from optical image (left) and SEM image (right) [126]. (d) Relationships between compressive strength and particle concentration [128]. (e) SEM image of a cell wall of particle reinforced ceramic foam and the relationships between strength and relative density of particulate ceramic foams produced by various techniques [128]. (f) The comparisons of strength among composite ceramic foams and particle reinforced alumina foams developed in [128]. (g) Comparison of composite ceramic foams with various mass ratio of compositions, where AS0, AS1, AS2, AS5 represent the alumina foam with silicon content of 0, 1, 2 and 5 wt%, respectively, and AS5B1, AS5B2, AS5B5 represent the additional wt% of boehmite powder [127].

Table 6. The compositions of each ceramic foams prepared by Liu et al. (2020).

Particles	Compositions (wt%)						
	AS0	AS1	AS2	AS5	AS5B1	AS5B2	AS5B5
Al_2O_3	100	99	98	95	94	93	90
Si	0	1	2	5	5	5	5
Boehmite	0	0	0	0	1	3	5

5. Multifunctionalities and applications of particle reinforced foams

The previous sections provide an overview of fabrication progress and mechanical properties of particle reinforced foams. The advantages of lightweight, ease of fabrication, good energy absorption etc. have made particle reinforced foams promising materials for numerous industrial fields. **Figs. 7a** to **d** show the actual applications of syntactic polymeric foams used in infrastructures (yellow pipelines), syntactic metal foams used in aircrafts (red components), in front bumper of vehicles, and in submarines, respectively. In addition to mechanical properties enhancement, adding various particles could either improve the existing functionalities or generate new features into the foams. In this section, the diverse functionalities of particle reinforced foams are highlighted, particularly focusing on thermal, electrical, acoustics, and self-healing properties. The applications correspond to the desired functionalities are also mentioned.

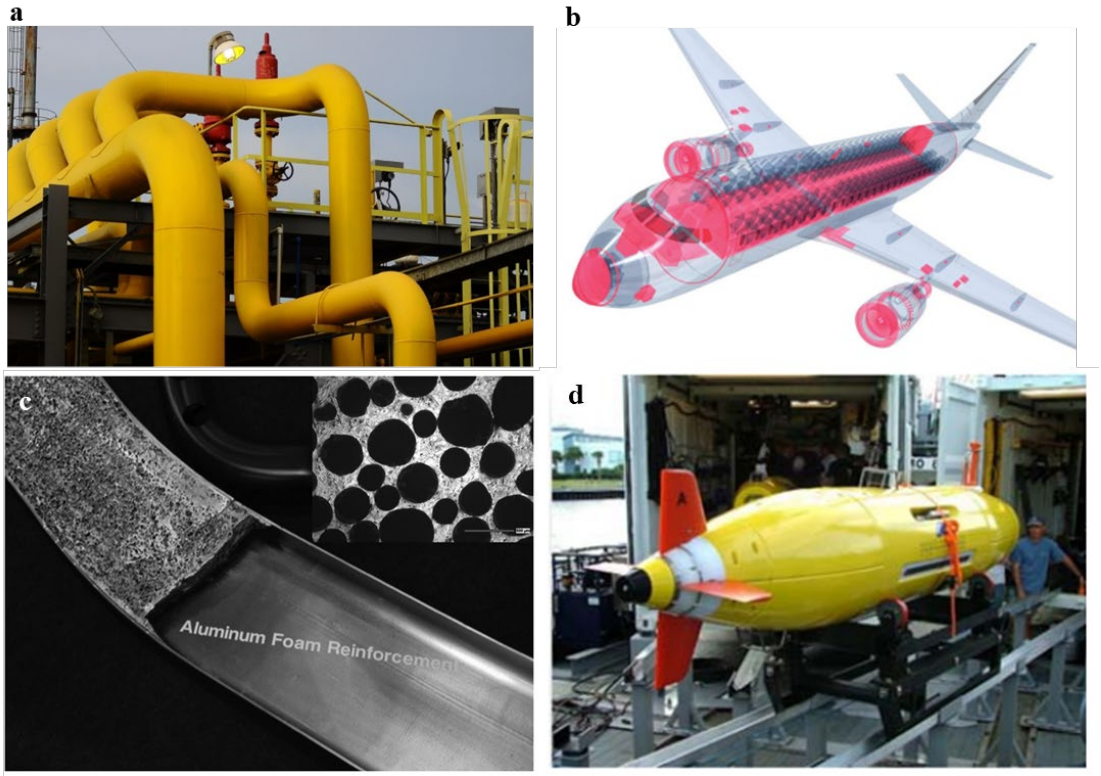

Figure 7 Particle reinforced foams used in real applications such as in (a) pipelines, (b) structural components in aircraft, (c) the front bumper of vehicle, and (d) submarine.

Thermal insulation and conductivity of particle reinforced foams

The requirements of thermal properties of particle reinforced foams are different depending on the specific applications. Excellent thermal insulation is essential for the foams used as the structural components in construction, aerospace, and marine fields [129-133]. Geng et al. (2016) investigated the heat insulation performances of polymer foams by adding hollow glass particles and B_4C microparticles [129]. An experimental setup is developed to test the heat-resistant performance, as shown in **Fig. 8a**. The results indicated the composite foams could withstand the flame temperature of 700 ^{0}C for over 300s without decreasing compressive strength. The heat-resistant mechanism was the transformation of B_4C to the glassy state B_2O_3, which promoted the bonding of hollow glass particles. Liu et al. (2018) added red mud microparticles into phenolic foams to improve mechanical properties and thermal insulation [130]. The experimental measurements indicated the thermal conductivity is decreased with the presence of particles, as shown as the plot in **Fig. 8b**. However, the thermal conductivity is increased dramatically when the particle contents are more than 15 wt%. The

modification of thermal property is induced by the chemical adhesion between particles and foam matrix. Then, Huang et al. (2018) embedded hollow glass particles into phenolic foams [131]. From the thermogravimetric analysis (TGA) results, the thermal conductivity was reduced after adding glass particles. With the increased content of glass particles, the flexural strength improved after various temperature treatments. Recently, Qiu et al. (2021) studied the thermal property of bamboo-based fiber particles reinforced polyurethane foams [132]. The experimental results revealed that the compressive strength, stiffness, and thermal stabilities were increased after adding fiber particles, which indicated the bamboo-based fiber particle reinforced polymer foams can be used as the structural components in thermal insulation in the infrastructure field.

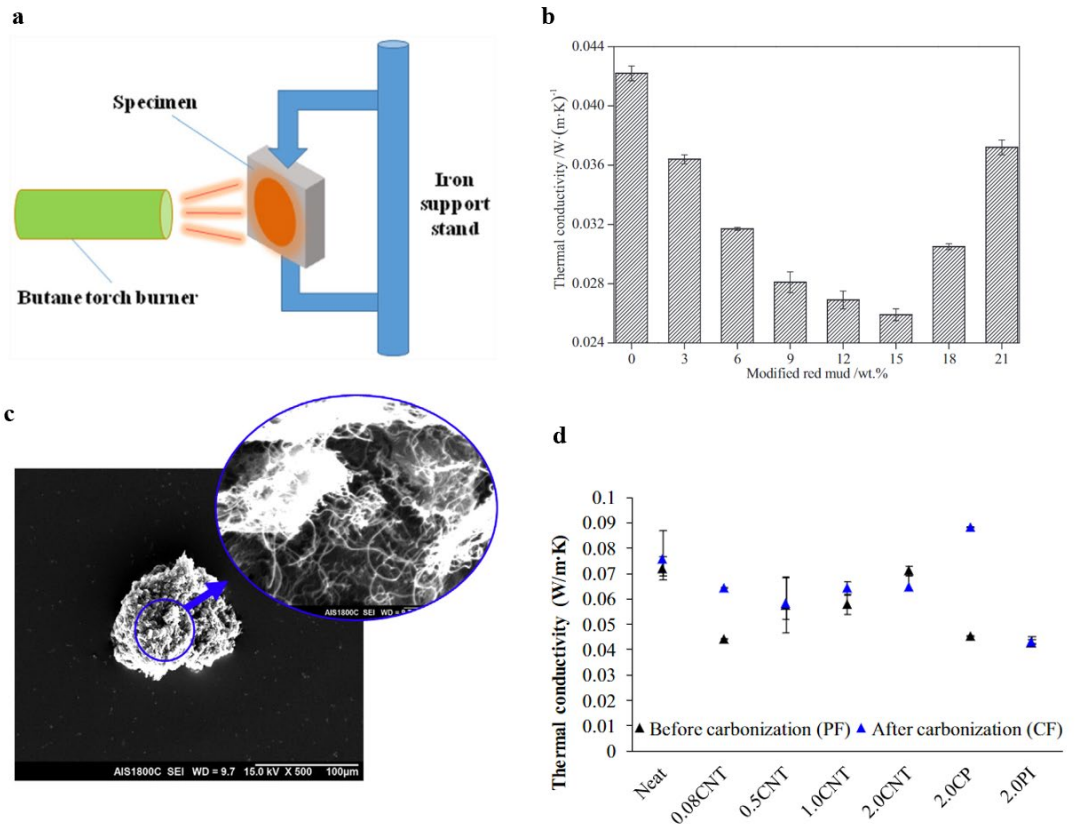

Figure 8 Thermal properties of particle reinforced foams. (a) Schematic illustration of an experimental setup for evaluating the heat-resistance performance of foams [129]. (b) Measurements of thermal conductivity of red mud particle reinforced foams [130]. (c) SEM image of a carbon particle added in phenolic foam for the improvement of thermal conductivity [134]. (d) Measurements of thermal conductivity of neat and carbon particle reinforced foams with a variety of particle contents [134].

In contrast to heat insulation, high thermal conductivity is beneficial to heat dissipation, which is an important physical property in integrated electronics [134-137]. To increase the thermal conductivity of foam, the thermally conductive particles have been added into the foam matrix during the high-temperature foaming process. Song et al. (2017) studied the thermal properties of carbonized phenolic foams reinforced by composite carbon particles [134]. The composite carbon particles (CP) were manufactured based on a polyimide varnish and multi-wall carbon nanotubes (MWCNT). The morphology of composite particles is shown in **Fig. 8c**. For the comparison purpose, neat polymer foam, polymer foams with various mass content of MWCNT, polymer foam with CP, and polymer foam with PI (polyimide) particles were manufactured. The measured thermal conductivity is shown in **Fig. 8d**, where the foams reinforced by 2.0 wt% CP present the highest thermal conductivity after carbonization. The compositions of reinforced foams are listed in **Table 7**. The improvement of thermal conductivity was induced by the transformation of polyimide into graphitic foam matrix after the carbonization, which formed a thermally conductive pathway. Then, Wu et al. (2020) added Al_2O_3 particles into the ceramic/polymer foam matrix, which significantly increased the thermal conductivity and flexural strength [135]. The ceramic particles under the high-temperature forming process formed strong chemical bonds with each other, and the phonon scattering at the interface was reduced. Therefore, continuous channels with good thermal conductivity were developed.

Table 7. Detail composition of particle reinforced foams reported by Song et al. (2017) [134], where CP, MWCNT, CF, and PI represents composite carbon particles, multi-wall carbon nanotubes, carbon foams, polyimide respectively.

Reinforced foam	Foam matrix	Particle content
CF	Phenolic foam	0 wt% MWCNT
CF_0.08CNT	Phenolic foam	0.08% wt% MWCNT
CF_0.5CNT	Phenolic foam	0.5% wt% MWCNT
CF_1.0CNT	Phenolic foam	1.0% wt% MWCNT
CF_2.0CNT	Phenolic foam	2.0% wt% MWCNT
CF_2.0CP	Phenolic foam	2.0% wt% CP
CF_2.0PI	Phenolic foam	2.0% wt% PI particle

Acoustic insulation of particle reinforced foams

Noise is a common hazard imposing psychological and physical effects on humans. Due to the excellent acoustic performances, foam materials have been used as the core materials of sandwich structures in constructions. There are two mechanisms contributing to the sound insulation of foam materials: The porous microstructure can dissipate sound wave energy through reflection and transformation to thermal energy, and the porous microstructure can eliminate the sound resonance [138-146]. Recently, some porous particles have been added into the foam matrix to promote the sound absorption capability. Meanwhile, mechanical properties have also been promoted. Chen and Jiang (2018) manufactured bamboo leaves particles reinforced polyurethane foams through direct stir casting [138]. A frequently-used experimental setup is employed to evaluate the sound transmission loss, as schematically shown in **Fig. 9a**. The measurements of transmission loss are shown in **Fig. 9b**. The polyurethane foam embedded with a 6% volume fraction of bamboo chips demonstrated the optimal transmission loss under the majority frequency range. The mechanism of sound wave loss was the promotion of sound reflection and resonance with the presence of bamboo particles within the foam matrix. Tiuc et al. (2019) fabricated a novel composite material based on the sawdust particles and polyurethane foam matrix [139]. In the previous researches, both porous materials have been proved to exhibit excellent sound absorption. The internal structure of a composite foam is shown in **Fig. 9c**. The composite foams with various particle contents were manufactured and tested by an experimental setup used for sound absorption coefficient measurement. The acoustic and mechanical experiments revealed that the sawdust particles could improve the tensile/compressive/bending strength and the sound absorption capability, except the frequency range of 2 kHz - 4 kHz. The enhancement of sound absorption was induced by the modifications of microstructure. The sawdust particles increased the airflow viscosity efficiently within the foam microstructure. Then, Zangiabadi and Hadianfard (2019) added hollow silica nanospheres into polyurethane foam to improve the sound absorption capability [140]. The shell of hollow nanospheres and the air trapped within the hollow particles caused the damping of sound waves. Besides, the sound energy

was dissipated by the thermal loss due to the friction between air molecules and cell walls. Muhazeli et al. (2020) fabricated the magnetorheological foams by adding carbonyl iron particles (CIPs) into a rigid polyurethane foam matrix [141]. The experimental results indicated that the sound absorption capability was tunable when the magnetic field was applied. The adjusting mechanism is schematically shown in **Fig. 9d**, which shows different channels transmission of sound waves under magnetic field. Recently, Lin et al. (2022) added hollow ceramic particles into the polyurethane foams to modify the mechanical properties and capability of sound absorption [143]. The coded name HCMF was the abbreviation of hollow ceramic microparticles reinforced foam, and the number after the HCMF was the volume fraction of microparticles. **Fig**. **9e** shows a sharp growth of compressive strength as a function of the HCMF content after HCMF15, where the trend is fluctuant before HCMF15.

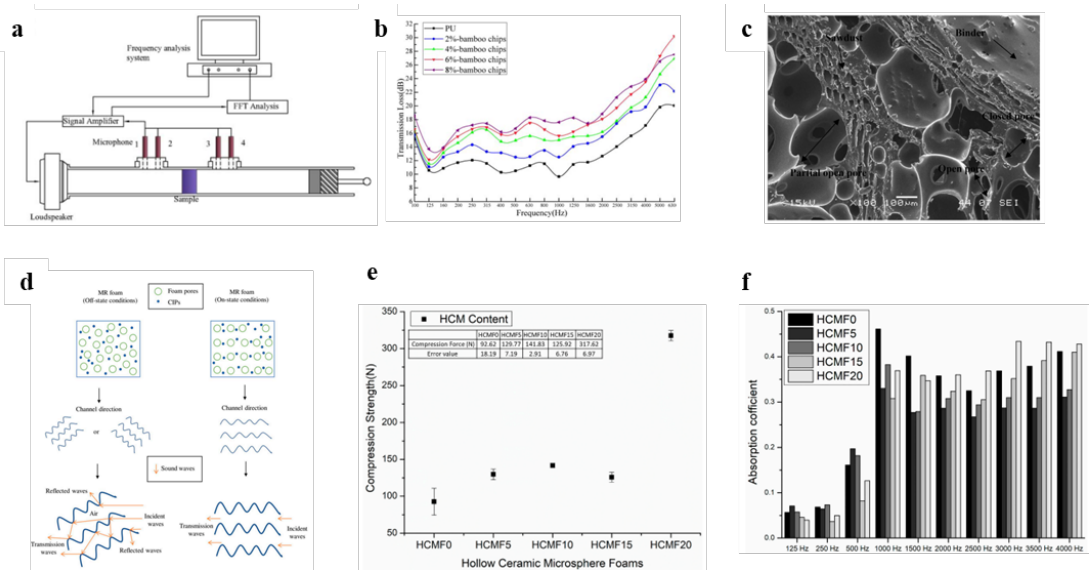

Figure 9 Acoustic properties of particle reinforced foams. (a) Schematic illustration of an experimental setup for evaluating the sound transmission loss of foams [138]. (b) Measurements of sound transmission loss of bamboo particles reinforced foams with various particle contents [138]. (c) Internal microstructure of sawdust particle reinforced foams used for sound insulation [139]. (d) Schematic drawing of modifying sound absorption capability of carbonyl iron particle reinforced polyurethane foam [141]. (e) Relationships between compressive strength and particle contents [143]. (f) Sound absorption capability of foams with various particle contents under different sound frequency (right plot), where HCMF represents the volume fraction of microparticles, and the numbers followed the abbreviation are the percentage of various volume fractions [143].

From **Fig. 9e**, the compressive strength of HCMF increases with more added microparticles. **Fig. 9f** shows the sound absorption coefficients of particle reinforced foams under various frequencies. From the measurements, the coefficients of different composite foams presented a steady increase with the rise of frequency, although the composite foams without and with low contents of particles (HCMF0, HCMF5, and HCMF10) showed higher coefficients at frequencies below 1000Hz, while HCMF15 and HCMF20 were more sensitive at higher frequencies. Liu et al. (2022) demonstrated that the average sound absorptivity of foam embedded with less content of particles was lower, which is induced by the sporadic distribution of particles within the foam matrix [145]. The inhomogeneous distribution could lead to a wide range of cell sizes. Aside from polymeric foams, the particle reinforced open-cell metal foams can also be used as sound absorbers, while the closed-cell metal foams present poor sound absorption performance [147]. The presence of particles within open-cell metal foam matrix enhances sound absorption capacity with additional energy dissipation at matrix-particles interfaces. For instance, Wu et al. (2003) demonstrated that embedding SiC_p particles in the aluminum foam matrix increased sound absorption properties, as the interfaces between Al and particles were beneficial to absorb the vibration energy [148].

Electrical properties of particle reinforced foams

In consideration of applications, the requirements of electrical properties of foam materials are various [35, 149-156]. Low dielectric constant materials play an essential role in the semiconductor field, decreasing the current leakage, the capacitance effect among wires, and the fever of integrated electronics. Polymer foams show a low dielectric constant due to the low polarizability of constituent materials and high porosity. Adding particles into the foam matrix can increase mechanical properties and control the dielectric constant. Shummugasamy et al. (2014) studied the electrical properties of hollow glass particles reinforced epoxy foams [151]. The internal microstructure of composite epoxy foam is shown in **Fig. 10a**. An experimental setup is developed to measure the impedance of foams, as shown in **Fig. 10b**, where the

dielectric constant could be calculated from the measured resistance. The results indicated that the dielectric constant could be tailored by modifying wall thickness and volume fraction of hollow particles. A theoretically linear expression was proposed to define the relationship between the dielectric constant and the density of foams. Then, Poveda and Gupta (2014) employed the Maxwell-Garnett and Jayasundere-Smith models to predict the dielectric constant of carbon nanofiber/hollow glass particles reinforced epoxy foams, which provided reasonable accuracy compared with experiments [152]. The theoretical and experimental results indicated that the impedance decreased and the dielectric constant increased with more carbon fiber contents. Besides, the impedance and dielectric constant can be controlled by the volume fraction and wall thickness of hollow particles. Ge et al. (2018) fabricated the ceramic/metal particles reinforced graphene foam based on the powder metallurgy technique for the potential application of porous electrodes [154]. After the solvothermal process, the 3D graphene network wrapped the particles to form a stable and homogenous internal structure, as shown in **Fig. 10c**. The presence of inorganic particles improved the mechanical properties of neat foams and increased electrical conductivity. Goodarzi et al. (2020) studied the mechanical and electrical properties of graphene particles reinforced linear and branched polypropylene foams [35]. Two different sizes of graphene particles (100 and 7 micrometers) were used as the particle additions. With the increase of graphene nanoparticles (GnP), the tensile modulus of foams increased gradually. The measured conductivity of solid graphene/polymer composites and composite foams is shown in **Fig. 10d**. The measurements indicated that the addition of graphene particles increased conductivity of different polymers and polymer foams apparently, as graphene particles altered the crystalline structure, decreased the spherulite size, and enhanced cell density.

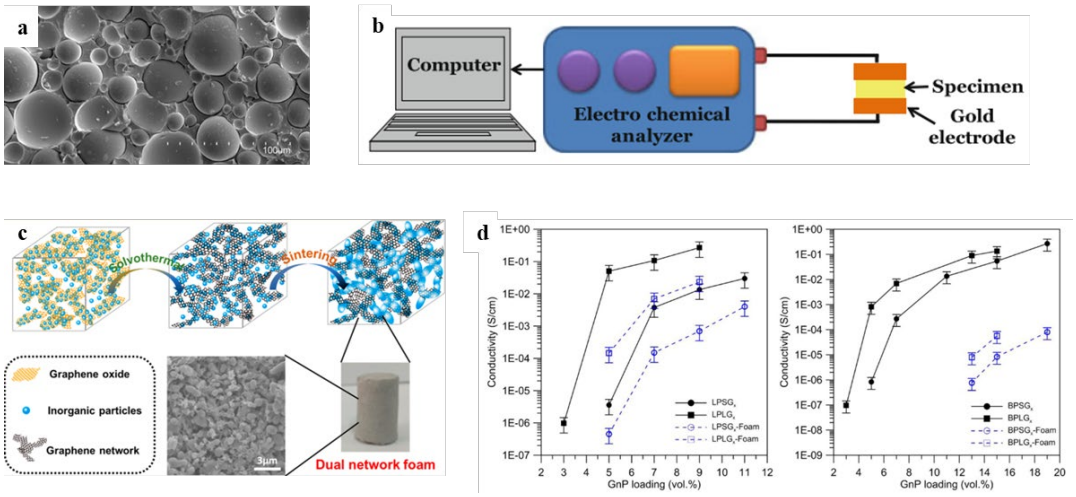

Figure 10 Electrical properties of particle reinforced foams. (a) SEM of cross-section of glass particle reinforced foams used for decreasing dielectric constant [151]. (b) Schematic illustration of experimental setup used for measuring the impedance of glass particle reinforced foams [151]. (c) Schematic drawing of 3D graphene-network wrapped particulate foam for the enhancement of electrical conductivity [154]. (d) Experimental measurements of electrical conductivity of solid graphene/polymer composites and composite foams. LPSG, LPLG, BPSG, and BPLG represent the small size graphene particles reinforced linear polymer, large size graphene particles reinforced linear polymer, small size graphene particles reinforced branched polymer, and large size graphene particles reinforced branched polymer, respectively, where GnP loading % represents the volume fraction of added graphene nanoparticles [35].

Self-healing of particle reinforced foams

As the foam core sandwich panels used in high-performance applications may be subject to a wide range of physical events, such as cyclic loadings, bird strikes, lightning strikes etc., the rapidly in-situ repairing of the damaged region is essential to avoid further damage to the whole structures [149, 157-163]. To overcome the limitations of the single-capsules self-healing system, Cao et al. (2019) fabricated bilayered capsules, incorporating two mutually reactive healing agents within the single capsule [157]. Then, the novel capsules were embedded into the epoxy foam matrix. The healing strategy is schematically shown in **Fig. 11a**. With the presence of capsules, the strength and modulus were both increased. Besides, the quasi-static compressive tests, three-point bending tests, and soft impact tests demonstrated that the bilayered capsules system provided multiple healing effects on the epoxy foams and the foam core sandwich beams [158]. Then, Cao and Liu (2021) proposed a numerical modelling framework to understand how healing agents flowed through the damaged foams and

influenced the mechanical responses under cyclic compressive tests [159]. To enable the simulations, a micromechanical model was developed to link damage to permeability of the cracked polymer foams as well as the saturation to the capillary pressure within the damaged polymer foams, as shown in **Fig. 11b**, where Ω(t) represents the volume occupied by a bulk foam material at the current configuration with the boundary SΩ(t) at time t under Cartesian coordinates $x1 - x2 - x3$; σ the effective stress tensor. The numerical modelling framework with the micromechanical model successfully captures the main features of the self-healing process, as shown in **Fig. 11c**, where the parameters of damage variable and saturation are used to evaluate the damage/healing effects and the amount of healing agents released from capsules. Zhan et al. (2021) manufactured the carbon nanotube wrapped expandable particles and added the particles into acrylic copolymer foams [162]. When the foam shows cracks, the inherent long-chain entanglements of carbon nanotube wrapped particles and acrylic copolymer foams provide the self-healing capability to the composite foam, as shown in **Fig. 11d**. Quadrini et al. (2021) investigated the shape memory polyurethane (PU) foam core sandwich beams with self-healing capabilities, where the microcapsules were used as the epoxy healing agent carriers [163]. The shape memory and healing effects are triggered by the heating process after damage, as schematically shown in **Fig. 11e**. The abbreviations of SM and SMPC shown in **Fig. 11e** are shape memory and shape memory polymer composite, respectively. Compared to the neat composite panels, the recovered stress/stiffness and shape recovery are more significant after embedding 0.5 wt% capsules, as shown in **Fig. 11f**.

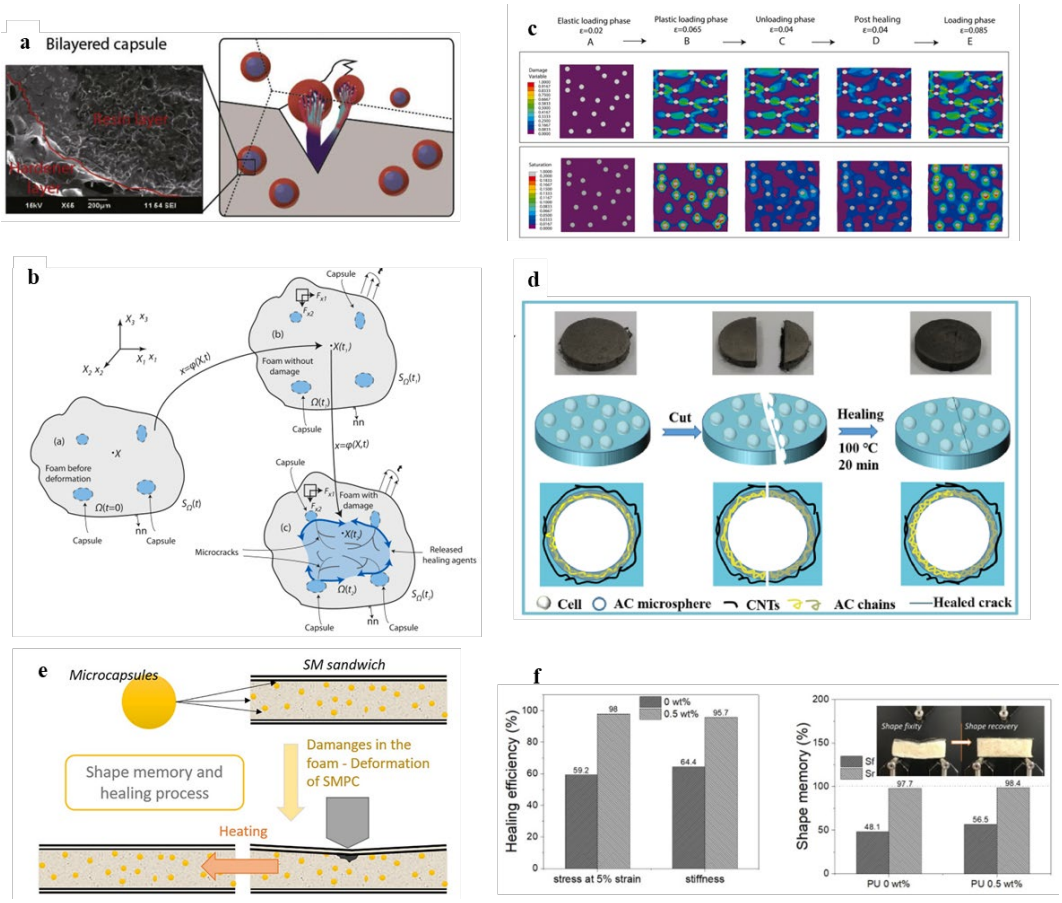

Figure 11 Self-healing of particle reinforced foams. (a) Schematic drawing of self-healing polymer foam with bilayered capsule system [157]. (b) Deformation mechanism of a foam embedded with capsules at initial, elastic, and damage configurations [159]. (c) FE simulation of self-healing process of bilayered capsules reinforced foams [159]. (d) Self-healing strategy of carbon nanotube wrapped expandable particulate acrylic copolymer foams [162]. (e) Self-healing strategy of shape memory PU foam structure embedded with self-healing capsules under three-point bending tests [163]. (f) The healing efficiency (left plot) and recovered fixity/shape (right plot) of neat foams and capsules embedded foam [163].

Electromagnetic interference shielding

Electromagnetic interference (EMI) shielding is the practice to reduce/block the electromagnetic field in a space with barriers. In recent years, the porous polymeric foams gradually replace the conducting metals with the advantages of light weight. To balance the weight and mechanical properties, the hollow particle reinforced foams are prepared and used in EMI shielding, where the hollow particles could be coated by conductive layer, or made by conductive materials [164,165]. For instance, Zhang et al. (2014) developed the hollow carbon particle reinforced epoxy foams, where the hollow

carbon particles were coated with poly-dopamine by self-polymerization of dopamine. The poly-dopamine provided the capability to enhance EMI shielding effectiveness of polymer foam [166]; Panigrahi et al. (2015) fabricated silver (Ag) coated polypyrrole microballoons. The EMI shielding effectiveness increased with the rise of Ag content. Such Ag coated hollow microballoons could be used as the filler material in syntactic foams [167]; Yu and Shen fabricated the Nickel coated cenospheres for the applications of EMI. The experimental results demonstrated that the coated cenospheres provided better EMI shielding effectiveness compared to the noncoated particles, indicating the promising alternative candidates for millimeter wave EMI shielding [168]. Aside from hollow particles, the nanoparticles have also been added in porous foams for EMI shielding. Yao et al. (2022) added hybrid nanofillers (i.e., nanoparticles and nanofibers) in Cu foams [169]. The composite foams can effectively shield the signal between Bluetooth earphone and smartphone, which posed the capability of EMI shielding in the fields of anti-monitoring and preventing cheating in exams.

Particle reinforced foam filled thin-walled structures

It is well-known that thin-walled structures, i.e., sandwich panels, engineered tubes, and among others, presents the advantages of light weight, excellent absorption capacity, and high crashworthiness [170]. Numerous research studies have been conducted on the performances of thin-walled structures filled with neat foams. The presence of particle reinforced foam matrix with the improvement of mechanical properties appeals great interests in engineered thin-walled structures in recent years.

Foam-core sandwich panels, consisting two thin/stiff panels and a thick foam core, are frequently used in industrial fields owing to the high stiffness-to-weight ratio [171]. In recent years, particle reinforced foam has been used as the core materials to replace neat foams, and the mechanical performances of composite sandwich panels have been investigated under various loading cases. Ahmadi et al. (2020) studied the impact behavior and failure mechanism of syntactic foam core composite sandwich panel [171], where the foam matrix was fabricated from a resin-hardener system, and three VF values of ceramic microballoons were adopted to make different specimens. The

ballistic impact tests were carried out at different impact velocities. The results indicated higher VF and smaller size of particles resulted in better ballistic resistance. Besides, the syntactic foam core provided limited failure area under impact loading compared to the neat foam core. Huang et al. (2020) studied the quasi-static and dynamic compressive responses of ceramic particle reinforced foam-filled corrugated sandwich panels [172]. The results indicated the higher VF of ceramic particles provided higher energy absorption capacity for sandwich panel under quasi-static compression. Pareta et al. (2020) investigated the shear modulus of fly ash particle reinforced polyurethane foams under three-point bending tests [173]. The results indicated the shear modulus of reinforced sandwich panel was increased up to 39% compared to the non-reinforced panels. From the outcomes of the above recent representative research, the addition of particles into foam cores provided better mechanical properties for sandwich panels.

Foam-core tube is a structural component providing good performance in energy absorbing under axial loading. While the large height-to-diameter/width ratio may cause instability, filling particles can effectively increase the bending stiffness of cross section [174]. Zhang et al. (2020) studied the energy absorption capacity of cenosphere reinforced foams under lateral quasi-static compression [175]. The particle reinforced foam-core tubes enhanced the mechanical performances dramatically, while the initial peak load and energy absorption increased with the decrease of the average particle size. In comparison, the increase of wall thickness led to the decrease of energy absorption capacity. Taherishargh et al. (2016) fabricated the steel tubes filled with porous expanded perlite particles reinforced foams. The energy absorption of tubes was improved compared to the neat tubes in both compressive and bending loading conditions [176]. As thin-walled tubes are the ideal choice as bumpers in automotive industry [177,178], the understanding of dynamic responses is significant before actual applications. For instance, Taherishargh et al. (2016) investigated the dynamic bending responses of expanded perlite particle reinforced metal foam filled steel tubes [179]. The foam filling increased the energy absorption capacity of tubes by 3.9 times, benefiting from the chemical reaction between the tubular shell and intermetallic

compound.

6. Conclusion, challenges, and future opportunities

This review focuses on the recent advances in particle reinforced foams, covering the manufacturing methods, mechanical properties, as well as the functionalities of particle additives and applications. The particle additives can enhance the mechanical properties and consequently increase the energy absorption capability effectively. In addition, particle additives can be used as the stabilizer during fabrication process. Compared to other composite foams, such as the fiber reinforced foams and nanotube reinforced foams, particle reinforced foams allow the large-scale production. Recent research progresses have revealed that additional functions, such as thermal/acoustic insulations, electric insulation/conductivity, and self-healing, could be endowed to the composite foams with the presence of particles. The advanced fabrication techniques and numerical modelling strategies have enabled tunable physical properties of particle reinforced foams by rational structural design. Thanks to their lightweight, good mechanical properties as well as tunable functionalities, particle reinforced foams have been intensively used in various civil and high-performance applications, ranging from constructions, infrastructures to automotive, aircrafts, submarines, and biomedical devices [2,5,10,180,183]. Despite significant progress summarized above, there still remains some challenges. The opportunities for future explorations of particle reinforced foams are elaborated in the below aspects:

1. **Fabrication techniques:** In the last decade, the syntactic foams have been applied in many applications benefiting from the gradually mature production technique. However, some fabricating issues still exist. For instance, the particle additives could hinder the development of regular and homogenous cellular structure during the foaming process. Besides, the mechanical properties of particle reinforced foams produced from conventional forming processes are isotropic, which is insufficient to fully exploit the reinforcing potential in complex loading conditions.

In recent years, researches have proposed the employment of a contactless magnetic field to build reinforcing structures in polymeric foams, which provided great potential in the acquiring of regular and homogenous cellular structure via the proper time-profile and intensity of a magnetic field during fabrication. The reinforcing direction can also be adjusted by modifying the magnetic field [184]. Another challenge is the large-scale fabrication of particle reinforced multifunctional foams. At present, the multifunctional foams can only be produced in small-scale in the lab. The major limitations with large-scale production are the repeatability and high cost for the civil and industrial purposes. To broaden the scope of applications, the advanced and economical production techniques of multifunctional foams should be developed in the first place [57,185-190]. The advanced additive manufacturing technique could be a promising solution for economic productions. Except for the 3D printing of thermoset foams [96,97], Bharath et al. (2020), Bharath et al. (2021), and Dileep et al. (2021) printed graded hollow glass particle reinforced thermoplastic foams via the fused filament fabrication (FFF) method. Compared to the conventional fabrication techniques, the FFF method showed the weight-saving potential of hollow glass particles in foam matrix between 9.27% and 28% [191-193].

2. **Mechanical properties and density:** The Ashby plots of the relationships between mechanical properties and density can be used to guide the selection of advanced materials in scientific and industrial fields [194-196]. In recent researches, the Young's modulus and strength of materials in common use are presented in the Ashby plots, as shown in **Fig. 12a** and **Fig. 12b**, respectively [197,198]. From the plots, the regions of foam materials are located at the left bottom, which show the characteristics of lightweight and weak mechanical properties. With the presence of particle additives, the mechanical properties are increased dramatically, however, the composite foams become heavier, such as the syntactic foams shown in Ashby plots in **Fig. 12c** and **Fig. 12d** [96]. As the weight of materials is the key property in some high-performance fields, the solid and porous particles become

unapplicable to achieve low density. In recent years, some novel ceramic and metal hollow particles with thinner shells have been developed. The advanced hollow particle reinforced foams achieve excellent ballistic impact and energy absorption compared to the control groups [171,199]. The future opportunities to achieve the particle reinforced foams with high mechanical properties and low density (circled regions shown in in **Fig. 12c** and **Fig. 12d)** could benefit from the development of hollow particles with thinner wall and relative higher strength [191,200-202].

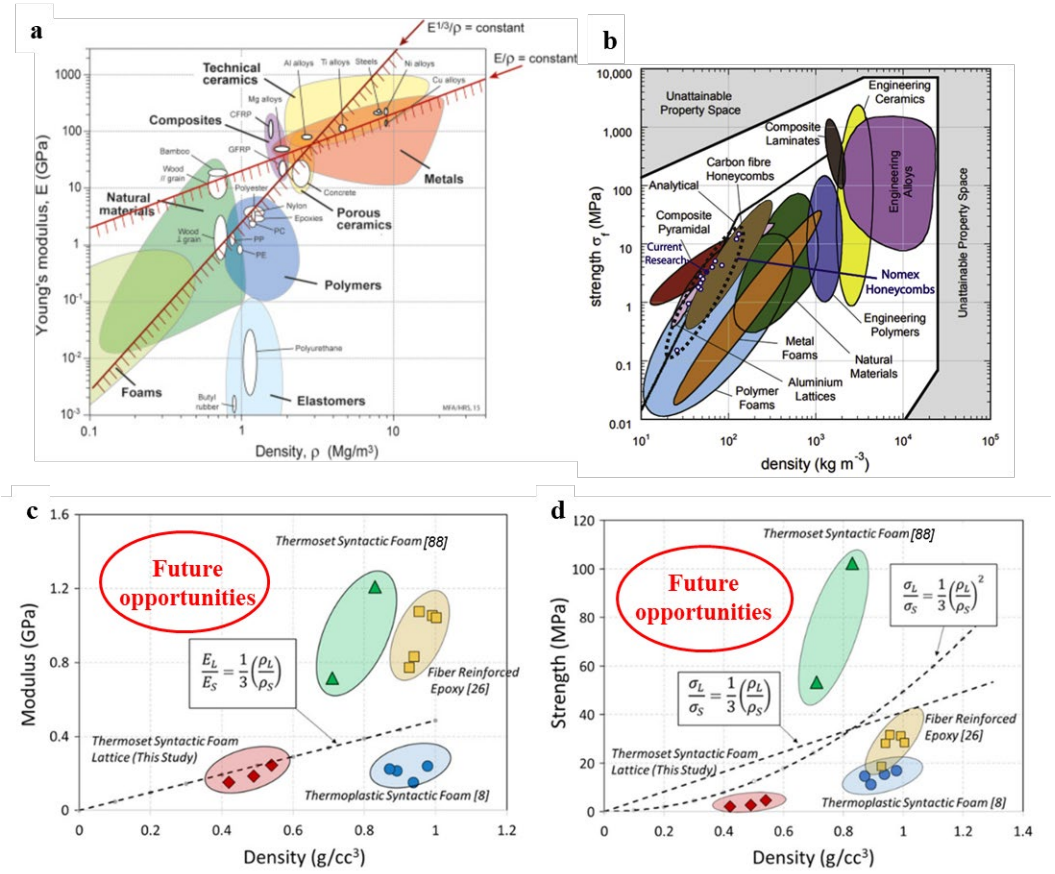

Figure 12 Ashby plots of foam materials. (a) and (b) Ashby plots of Young's modulus and strength of materials in common use, respectively [197,198]. (c) and (d) Ashby plots of mechanical properties of a variety of syntactic foams under compressions [96].

3. **Modelling strategies:** The full-scale FE models, such as 3D Voronoi model, Kevin model have been widely used to analyze the mechanical performance of foams with high accuracy [203-205]. In order to reduce computational costs, the representative volume element (RVE) technique have been applied by existing researches to avoid full-scale simulations of foams and particle reinforced foams [206-212]. Owing to

the stochastic nature of internal structure of foams, the cells and particle reinforcements may not follow the periodic distribution with a unit size. Thus, the deformation mechanism may not be captured accurately due to the local simulation. Cao et al. (2021) proposed an approximate strategy to create hollow cells in a relatively heavier foam matrix to represent the lightweight foam matrix to ensure the same density [213]. This strategy has been used for the full-scale simulations of porous particle reinforced foams under quasi-static and dynamic compressions [106,213]. The deformation and reinforcing mechanisms of particle reinforced foams have been successfully captured with explicitly modelling of particles and hollow cells. However, the accuracy of stiffness is least desirable due to the coarse treatment of the interface between particles and cell structures, where the serious interfacial debonding occurred at a high strain rate. To deal with this problem, Carolan et al. (2020) used cohesive element at interfaces between particles and foam matrix. Both elastic modulus and tensile strength have been reasonable predicted, while the particles were modelled explicitly [214]. In the theoretical modelling strategy, Prabhakar et al. (2022) built a 2D micromechanical model to understand the mechanical properties of syntactic polymer foams [215]. The theoretical framework with the combination of computational models and multiple linear regression analysis provided analytical solutions to the mechanical properties of syntactic foams, which are influenced by the particle volume fraction, particle wall thickness, bonding between the particle, and the matrix etc. In the future modelling work of particle reinforced foams, a comprehensive strategy could be developed considering the recent progress.

4. **Novel application fields:** In conventional applications, foams are often used as the structural components. Although the foams have endowed additional functions with the presence of particle additives, such as thermal conductivity, acoustic insulation etc. [148,170,216-222], the role of foams are still focused in the structural fields. For instance, Chen et al. (2022) added various volume fractions of silica aerogel particles into geopolymer foam. The composite foams endowed

both super thermal insulating and excellent sound absorption, which showed great potential in building materials for energy saving [223]. In recent years, several researchers explored novel application fields of particle reinforced foams in healthcare and electrical fields [224,225]. Lin et al. (2022) developed the dual functionalisation of polyurethane foams with the presence of metal particles. Except for the reinforcing function, the metal particles showed the property of antibacterial and flame retardance [224]. In this case, the metal particle reinforced foams show the potential in healthcare fields. Besides, Sun et al. (2022) fabricated the FeOx-based particulate nickel foams [225]. The Fe_2O_3 and Fe_3O_4 anode materials using the Fe-based metal-organic in the nickel foam matrix exhibited high energy density, which showed the promising applications in energy storage devices. In the future opportunities, the explorations of particle reinforced foams could be carried out in more novel applications. For instance, the porous structure of foams could be added with some biological cues. The porous microarchitecture can provide the microenvironment for cells adhesion and transition. The biological stimulations could enhance the cells differentiation and tissue regeneration.

Declaration of Competing Interest

There is no competing financial interest or personal relationship that could have appeared to influence the work reported in this article.

Acknowledgements

S.C. gratefully acknowledges the support of National Natural Science Foundation of China (Grant. No. 12102220). R.B. gratefully acknowledges the support of the National Natural Science Foundation of China (Grant. No. 12102221). R.B. gratefully acknowledges the support of the Office of China Postdoc Council (OCPC) and Tsinghua University for the International Postdoctoral Exchange Fellowship Program (Talent-Introduction Program) YJ20200112. R.B. gratefully acknowledges the support of China Postdoctoral Science Foundation for the fellowship (2021M691795).

References

[1] Le D, Novak N, Arjunan A, Baroutaji A, Estrada Q, Tran T, Le H. Crashworthiness of bio-inspired multi-stage nested multi-cell structures with foam core. Thin Wall Struct 2023;182, Part A:110245. https://doi.org/10.1016/j.tws.2022.110245.
[2] Cao SZ, Liu T, Jones A, Tizani W. Particle reinforced thermoplastic foams under quasi-static compression. Mech Mater 2019;103081. doi.org/10.1016/j.mechmat.2019.103081.
[3] Fang B, Huang W, Xu H, Jiang C, Liu, J. High-velocity impact resistance of stepwise gradient sandwich beams with metal foam cores. Thin Wall Struct 2022; 181:110054. https://doi.org/10.1016/j.tws.2022.110054.
[4] Afolabi LO, Ariff ZM, Hashim SFS, Alomayri T, Mahzan S, Kamarudin KA, et al. Syntactic foams formulations, production techniques, and industry applications: a review. J Mater Res Technol. 2020;9:10698-10718. doi.org/10.1016/j.jmrt.2020.07.074.
[5] Szklarek K, Kotelko M, Ferdynus M. Crashworthiness performance of thin-walled hollow and foam-filled prismatic frusta - FEM parametric studies - Part 1. Thin Wall Structs 2022;181:110046. https://doi.org/10.1016/j.tws.2022.110046.
[6] Banhart J, Manufacturing, characterisation and application of cellular metals and metal foams. Prog. Mater. Sci. 2001;46:559-632.
[7] Chen J, Zhu L, Fang H, Han J, Huo R, Wu P. Study on the low-velocity impact response of foam-filled multi-cavity composite panels. Thin Wall Struct 2022;173:108953. https://doi.org/10.1016/j.tws.2022.108953.
[8] Liu J, Yang W, Liu J, Liu, J, Huang W. Ballistic impact analyses of foam-filled double-arrow auxetic structure. Thin Wall Struct 2023;182, Part A:110173. https://doi.org/10.1016/j.tws.2022.110173.
[9] Du L, Jiao GQ. Indentation study of Z-pin reinforced polymer foam core sandwich structures. Compos Part A Appl Sci 2009;40:822-829. doi.org/10.1016/j.compositesa.2009.04.004.
[10] Kaczynski P, Ptak M, Gawdzinska K. Energy absorption of cast metal and composite foams tested in extremely low and high-temperatures. Mater Des 2020;196:109114. doi.org/10.1016/j.matdes.2020.109114.
[11] Monno M, Negri D, Mussi V, Aghaei P, Groppi G, Tronconi E, et al. Cost-Efficient Aluminum Open-Cell Foams: Manufacture, Characterization, and Heat Transfer Measurements. Adv Engin Mater. 2018;20:1701032. doi.org/10.1002/adem.201701032.
[12] Raj RE, Parameswaran V, Daniel BSS. Comparison of quasi-static and dynamic compression behavior of closed-cell aluminum foam. Mat Sci Eng A-Struct 2009;526:11-15. doi.org/10.1016/j.msea.2009.07.017.
[13] Wang NZ, Maire E, Chen X, Adrien J, Li YX, Amani Y, et al. Compressive performance and deformation mechanism of the dynamic gas injection aluminum foams. Mater Charact 2019;147:11-20. doi.org/10.1016/j.matchar.2018.10.013.
[14] Noack MA, Bulk F, Wang NZ, Banhart J, Garcia-Moreno F. Aluminium foam with sub-mm sized cells produced using a rotating gas injector. Mater Sci Eng B-Adv 2021;273:115427. doi.org/10.1016/j.mseb.2021.115427.
[15] Bo CY, Yang XH, Hu LH, Zhang M, Jia PY, Zhou YH. Enhancement of flame-

retardant and mechanical performance of phenolic foam with the incorporation of cardanol-based siloxane. Polym Compos 2019;40:2539-2547. doi.org/10.1002/pc.25285.
[16] Barzigar SS, Ahmadi H, Liaghat G. An analytical investigation on crushing behavior of thin-walled tubes filled with a foam with strain hardening region. Thin Wall Struct 2023;182, Part A: 110169. https://doi.org/10.1016/j.tws.2022.110169.
[17] Hou JJ, Zhao GQ, Wang GL, Dong GW, Xu JJ. A novel gas-assisted microcellular injection molding method for preparing lightweight foams with superior surface appearance and enhanced mechanical performance. Mater Des 2017;127:115-125. doi.org/10.1016/j.matdes.2017.04.073.
[18] Li H, Li Z, Xiao Z, Xiong J, Wang X, Han Q, Zhou J, Guan Z. Vibro-impact response of FRP sandwich plates with a foam core reinforced by chopped fiber rods. Compos B Eng 2022;242:110077. doi.org/10.1016/j.compositesb.2022.110077.
[19] Rice MC, Fleischer CA, Zupan M. Study on the collapse of pin-reinforced foam sandwich panel cores. Exp Mech 2006;46:197-204. doi.org/10.1007/s11340-006-7103-3.
[20] Zegeye EF, Woldesenbet E. Processing and mechanical characterization of carbon nanotube reinforced syntactic foams. J Reinf Plast Compos 2012;31:1045-1052. doi.org/10.1177/0731684412452919.
[21] Orbulov IN, Szlancsik A, Kemeny A, Kincses D. Compressive mechanical properties of low-cost, aluminium matrix syntactic foams. Compos Part A Appl Sci 2020;135. doi.org/10.1016/j.compositesa.2020.105923.
[22] Orbulov IN. Metal matrix syntactic foams produced by pressure infiltration-The effect of infiltration parameters. Mat Sci Eng A-Struct 2013;583:11-19. doi.org/10.1016/j.msea.2013.06.066.
[23] Yousaf Z, Smith M, Potluri P, Parnell W. Compresion properties of polymeric syntactic foam composites under cyclic loading. Compos B Eng. 2020;186:107764. doi.org/10.1016/j.compositesb.2020.107764.
[24] Hajimohammadi A, Ngo T, Provis JL, Kim T, Vongsvivut J. High strength/density ratio in a syntactic foam made from one-part mix geopolymer and cenospheres. Compos B Eng 2019;173:106908. doi.org/10.1016/j.compositesb.2019.106908.
[25] Yuan J, An ZG, Zhang JJ. Effects of hollow microsphere surface property on the mechanical performance of high strength syntactic foams. Compos Sci Technol. 2020;199:108309. doi.org/10.1016/j.compscitech.2020.108309.
[26] Singh AK, Deptula AJ, Anawal R, Doddamani M, Gupta N. Additive Manufacturing of Three-Phase Syntactic Foams Containing Glass Microballoons and Air Pores. JOM. 2019;71:1520-1527. doi.org/10.1007/s11837-019-03355-5.
[27] Spowart JE, Gupta N, Lehmhus D. Additive Manufacturing of Composites and Complex Materials. JOM. 2018;70:272-274. doi.org/10.1007/s11837-018-2742-2.
[28] Valdez M, Kozuch C, Faierson EJ, Jasiuk I. Induced porosity in Super Alloy 718 through the laser additive manufacturing process: Microstructure and mechanical properties. J Alloy Compd. 2017;725:757-764. doi.org/10.1016/j.jallcom.2017.07.198.
[29] Afolabi LO, Mutalib NAA, Ariff ZM. Fabrication and characterization of two-phase syntactic foam using vacuum assisted mould filling technique. J Mater Res

Technol. 2019;8:3843-3851. doi.org/10.1016/j.jmrt.2019.06.046.
[30] Cheneler D, Kennedy AR. A comparison of the manufacture and mechanical performance of porous aluminium and aluminium syntactic foams made by vacuum-assisted casting. Mat Sci Eng A-Struct 2020;789:139528. doi.org/10.1016/j.msea.2020.139528.
[31] Balch DK, Fitzgerald TJ, Michaud VJ, Mortensen A, Shen YL, Suresh S. Thermal expansion of metals reinforced with ceramic particles and microcellular foams. Metall Mater Trans A: Phys Metall Mater Sci 1996;27:3700-3717. doi.org/10.1007/BF02595462.
[32] Labella M, Zeltmann SE, Shunmugasamy VC, Gupta N, Rohatgi PK. Mechanical and thermal properties of fly ash/vinyl ester syntactic foams. Fuel 2014;121:240-249. doi.org/10.1016/j.fuel.2013.12.038.
[33] Scarpa F, Bullough WA, Lumley P. Trends in acoustic properties of iron particle seeded auxetic polyurethane foam. Proc Inst Mech Eng Part C 2004;218:241-244. doi: 10.1243/095440604322887099
[34] Olcay H, Kocak ED. Rice plant waste reinforced polyurethane composites for use as the acoustic absorption material. Appl Acoust 2021;173:107733. doi.org/10.1016/j.apacoust.2020.107733
[35] Goodarzi V, Fasihi M, Garmabi H, Ohshima M, Taki K, Saeb MR. Microstructure, mechanical and electrical characterizations of bimodal and nanocellular polypropylene/graphene nanoplatelet composite foams. Mater Today Commun 2020;25:101447. doi.org/10.1016/j.mtcomm.2020.101447
[36] Zegeye E, Wicker S, Woldesenbet E. AC and DC electrical properties of graphene nanoplatelets reinforced epoxy syntactic foam. Mater Res Express 2018;5:045605. doi.org/10.1088/2053-1591/aabbfd.
[37] Kanu NJ, Gupta E, Vates UK, Singh GK. Self-healing composites: A state-of-the-art review. Compos Part A Appl Sci 2019;121:474-486. doi.org/10.1016/j.compositesa.2019.04.012.
[38] Jayabalakrishnan D, Muruga DBN, Bhaskar K, Pavan P, Balaji K, Rajakumar PS, et al. Self-Healing materials-A review. Mater Today Proc 2021;45:7195-7199. doi.org/10.1016/j.matpr.2021.02.415.
[39] Muhazeli NS, Nordin NA, Mazlan SA, Rizuan N, Aziz SAA, Abd Fatah AY, et al. Characterization of morphological and rheological properties of rigid magnetorheological foams via in situ fabrication method. J Mater Sci 2019;54:13821-13833. doi.org/10.1007/s10853-019-03842-9.
[40] Kumar BRB, Doddamani M, Zeltmann SE, Gupta N, Ramesh MR, Ramakrishna S. Processing of cenosphere/HDPE syntactic foams using an industrial scale polymer injection molding machine. Mater Des 2016;92:414-423. doi.org/10.1016/j.matdes.2015.12.052.
[41] Banhart J, Manufacturing routes for metallic foams. JOM 2000;52:22-27. doi.org/10.1007/s11837-000-0062-8.
[42] Banhart J, Light-metal foams-History of innovation and technological challenges. Adv. Eng. Mater. 2012;15:82-111. doi.org/10.1002/adem.201200217.
[43] Liu JG, He SY, Zhao H, Li G, Wang MY. Experimental investigation on the

dynamic behaviour of metal foam: From yield to densification. Int J Impact Eng 2018;114:69-77. doi.org/10.1016/j.ijimpeng.2017.12.016.
[44] Alteneiji M, Krishnan K, Guan ZW, Cantwell WJ, Zhao Y, Langdon G. Dynamic responses of aluminium matrix syntactic foams subjected to high-rate loadings. Compos Struct 2023; 303:116289. doi.org/10.1016/j.compstruct.2022.116289.
[45] Elbir S, Yilmaz S, Toksoy AK, Guden M. SiC-particulate aluminum composite foams produced by powder compacts: Foaming and compression behavior. J Mater Sci 2003;38:4745-4755. doi: 10.1023/A:1027427102837.
[46] He S, Carolan D, Fergusson A, Taylor AC. Toughening epoxy syntactic foams with milled carbon fibres: Mechanical properties and toughening mechanisms. Mater. Des. 2019; 107654. doi.org/10.1016/j.matdes.2019.107654.
[47] Uzun A. Production of aluminium foams reinforced with silicon carbide and carbon nanotubes prepared by powder metallurgy method. Compos B Eng 2019;172:206-217. doi.org/10.1016/j.compositesb.2019.05.045.
[48] Anbuchezhiyan G, Mohan B, Karthikeyan RV. Development of magnesium matrix syntactic foams processed through powder metallurgy techniques. Appl Mech Mater. 2015;766-767:281-286. doi.org/10.4028/www.scientific.net/AMM.766-767.281.
[49] Vogiatzis CA, Tsouknidas A, Kountouras DT, Skolianos S. Aluminum-ceramic cenospheres syntactic foams produced by powder metallurgy route. Mater Des. 2015;85:444-454. doi.org/10.1016/j.matdes.2015.06.154.
[50] Song YH, Tane M, Ide T, Seimiya Y, Hur BY, Nakajima H. Fabrication of Al-3.7 Pct Si-0.18 Pct Mg Foam Strengthened by AlN Particle Dispersion and its Compressive Properties. Metall Mater Trans A: Phys Metall Mater Sci 2010;41:2104-2111. doi.org/10.1007/s11661-010-0247-x.
[51] Khare S. Sorte M. An Overview of Aluminum Foam Production Methods. Int J Eng Sci 2021;11:27659-27666.
[52] de la Muela AMS, Duarte J, Baptista JS, Cambronero LEG, Ruiz-Roman JM, Elorza FJ. Stir Casting Routes for Processing Metal Matrix Syntactic Foams: A Scoping Review. Process 2022;10:478. doi.org/10.3390/pr10030478.
[53] Sunar T, Cetin M. Manufacturing of B4C particle reinforced A360 aluminium cellular composite materials by the integration of stir casting and space holder methods. J Compos Mater. 2021;55:3763-3773. doi.org/10.1177/00219983211022825.
[54] Daoud A. Synthesis and characterization of novel ZnAl22 syntactic foam composites via casting. Mat Sci Eng A-Struct 2008;488:281-295. doi.org/10.1016/j.msea.2007.11.020.
[55] Meng J, Liu TW, Wang HY, Dai LH. Ultra-high energy absorption high-entropy alloy syntactic foam. Compos B Eng. 2021; 207:108563. doi.org/10.1016/j.compositesb.2020.108563.
[56] Szlancsik A, Katona B, Bobor K, Majlinger K, Orbulov IN. Compressive behaviour of aluminium matrix syntactic foams reinforced by iron hollow spheres. Mater Des 2015;83:230-237. doi.org/10.1016/j.matdes.2015.06.011.
[57] Brothers AH, Dunand DC. Syntactic bulk metallic glass foam. Appl Phys Lett 2004;84:1108. doi.org/10.1063/1.1646467
[58] Li YC, Xiong JY, Lin JG, Forrest M, Hodgson PD, Wen CE. Mechanical properties

and energy absorption of ceramic particulate and resin-impregnation reinforced aluminium foams. Mater Forum 2007;31:52-56. hdl.handle.net/1959.3/93150
[59] Wichianrat E, Boonyongmaneerat Y, Asavavisithchai S. Microstructural examination and mechanical properties of replicated aluminium composite foams. Tran Nonferrous Met Soc China. 2012;22:1674-1679. doi.org/10.1016/S1003-6326(11)61372-1.
[60] Kulshreshtha A, Dhakad SK, Mondal DP. Effect of particle size on compressive deformation of Aluminium foam prepared through stir casting technique. Mater Today Proc 2021;47:7174-7177. doi.org/10.1016/j.matpr.2021.06.384.
[61] Liu J, Yu SR, Zhu XY, Wei M, Luo YR, Liu YH. Correlation between ceramic additions and compressive properties of Zn-22Al matrix composite foams. J Alloys Compd 2009;476:220-225. doi: 10.1016/j.jallcom.2008.09.069
[62] Broxtermann S, Su MM, Hao H, Fiedler T. Comparative study of stir casting and infiltration casting of expanded glass-aluminium syntactic foams. J Alloys Compd 2020;845:155415. doi.org/10.1016/j.jallcom.2020.155415
[63] Kannan S, Kishawy HA, Pervaiz S, Thomas K, Karthikeyan R, Arunachalam R. Machining of novel AA7075 foams containing thin-walled ceramic bubbles. Mater Manuf Process 2020;35:181218-21. doi.org/10.1080/10426914.2020.1802038.
[64] Movahedi N, Vesenjak M, Belova IV, Murch GE, Fiedler T. Dynamic compression of functionally-graded metal syntactic foams. Compos Struct 2021;261:113308. doi.org/10.1016/j.compstruct.2020.113308.
[65] Yang QZ, Cheng JC, Wei YP, Yu B, Miao ZQ, Gao P. Innovative compound casting technology and mechanical properties of steel matrix syntactic foams. J Alloys Compd 2021;853:156572. doi.org/10.1016/j.jallcom.2020.156572.
[66] Karoly D, Iklodi Z, Kemeny A, Kincses DB, Orbulov IN. Production and Functional Properties of Graded Al-Based Syntactic Metal Foams. Metals. 2022;12:263. doi.org/10.3390/met12020263.
[67] Taherishargh M, Linul E, Broxtermann S, Fiedler T. The mechanical properties of expanded perlite-aluminium syntactic foam at elevated temperatures. J. Alloys Compd 2018;737:590-596.
[68] Fiedler T, Al-Sahlani K, Linul PA, Linul E. Mechanical properties of A356 and ZA27 metallic syntactic foams at cryogenic temperature. J. Alloys Compd 2020;813:152181. doi.org/10.1016/j.jallcom.2019.152181. doi.org/10.1016/j.jallcom.2017.12.083
[69] Kemeny A, Katona B, Movahedi N, Fiedler T. Fatigue tests of zinc aluminium matrix syntactic foams filled with expanded perlite. IOP Conf. Ser.: Mater. Sci. Eng. 2020; 903:012050. **doi**.10.1088/1757-899X/903/1/012050
[70] Movahedi N, Taherishargh M, Belova IV, Murch GE, Fiedler T. Mechanical and microstructures characterization of an AZ91-activated carbon syntactic foam. Materials 2019;12(1):3. doi:10.3390/ma12010003
[71] Movahedi N, Murch GE, Belova IV, Fiedler T. Functionally graded metal syntactic foam: Fabrication and mechanical properties. Mater. Des. 2019;168:107652. doi.org/10.1016/j.matdes.2019.107652.
[72] Su M, Wang H, Hao H, Fiedler T. Compressive properties and expanded glass and

alumina hollow spheres hybrid reinforced aluminum matrix syntactic foams. 2020;821:153233. doi.org/10.1016/j.jallcom.2019.153233.
[73] Gupta N, Pinisetty D, Shunmugasamy VC, Gupta N, Pinisetty D, Shunmugasamy VC. Introduction. In: Reinforced Polymer Matrix Syntactic Foams. SpringerBriefs in Materials. Springer, Cham. 2013. doi.org/10.1007/978-3-319-01243-8_1
[74] Ou A, Huang Z, Qin R, Chen X, Li Y, Liu Y, et al. Preparation of Thermosetting/Thermoplastic Polyimide Foam with Pleated Cellular Structure via In Situ Simultaneous Orthogonal Polymerization. ACS Appl Polym Mater. 2019;1:2430-2440. doi.org/10.1021/acsapm.9b00558.
[75] Pinisetty D, Shunmugasamy VC, Gupta N. Hollow Glass Microspheres in Thermosets—Epoxy Syntactic Foams. In Plastics Design Library, Hollow Glass Microspheres for Plastics, Elastomers, and Adhesives Compounds, William Andrew Publishing, 2015;147-174. doi.org/10.1016/B978-1-4557-7443-2.00006-2.
[76] Qi C, Yu Q, Zhao Y. Fabrication and characterization of the thermoplastic and thermoset syntactic foam core-based sandwich composites. Polym Compos 2020;41:3052-3061. doi.org/10.1002/pc.25597.
[77] Ding J, Ye F, Liu Q, Yang C, Gao Y, Zhang B. Co-continuous hollow glass microspheres/epoxy resin syntactic foam prepared by vacuum resin transfer molding. J Reinf Plast Compos 2019;38:896-909. doi.org/10.1177/0731684419857173.
[78] Swetha C, Kumar R. Quasi-static uni-axial compression behaviour of hollow glass microspheres/epoxy based syntactic foams. Mater Des 2011;32:4152-4163. doi.org/10.1016/j.matdes.2011.04.058.
[79] Wu X, Dong L, Zhang F, Zhou Y, Wang L, Wang D, et al. Preparation and characterization of three phase epoxy syntactic foam filled with carbon fiber reinforced hollow epoxy macrospheres and hollow glass microspheres. Polym Compos 2016;37:497-502. doi.org/10.1002/pc.23205.
[80] Jiang T, Gao Y, Wang Y, Zhao Z, Yu J, Yang K, et al. Development and Mechanical Characterization of HGMS-EHS-Reinforced Hollow Glass Bead Composites. ACS Omega 2020;5:6725-6737. doi.org/10.1021/acsomega.0c00015.
[81] Yu Q, Zhao Y, Dong A, Li Y. Mechanical properties of EPS filled syntactic foams prepared by VARTM. Compos B Eng 2018;136:126-134. doi.org/10.1016/j.compositesb.2017.07.053.
[82] Kumar BRB, Zeltmann SE, Doddamani M, Gupta N, Uzma, Gurupadu S, et al. Effect of cenosphere surface treatment and blending method on the tensile properties of thermoplastic matrix syntactic foams. J Appl Polym Sci 2016;133:43881. doi.org/10.1002/app.43881.
[83] Shutov FA. Syntactic polymer foams. In: Chromatography/Foams/Copolymers. Adv Polym Sci Springer, Berlin, Heidelberg 1986. doi.org/10.1007/3-540-15786-7_7.
[84] Wu G, Xie P, Yang H, Dang K, Xu Y, Sain M, et al. A review of thermoplastic polymer foams for functional applications. J Mater Sci. 2021;56:11579-11604. doi.org/10.1007/s10853-021-06034-6.
[85] Valentina V, Auria MD, Sorrentino L, Daniele D, Pantani R. Foam injection molding of magneto sensitive polymer composites. Sens Actuator A Phys

2022;337:113427. doi.org/10.1063/1.5084844.
[86] Volpe V, D'Auria M, Sorrentino L, Davino D, Pantani R. Magneto-mechanical behavior of elastomeric carbonyl iron particles composite foams produced by foam injection molding. J Magn Magn Mater 2018;466:44-54. doi.org/10.1016/j.jmmm.2018.06.071.
[87] Qi CJ, Yu QY, Zhao Y. Fabrication and characterization of the thermoplastic and thermoset syntactic foam core-based sandwich composites. Polym Compos 2020;41:3052-3061. doi: 10.1002/pc.25597305.
[88] Wu H, Zhao GQ, Wang GL, Zhang WL, Li Y. A new core-back foam injection molding method with chemical blowing agents. Mater Des 2018;144:331-342. doi.org/10.1016/j.matdes.2018.02.043.
[89] Kharbas HA, McNulty JD, Ellingham T, Thompson C, Manitiu M, Scholz G, et al. Comparative study of chemical and physical foaming methods for injection-molded thermoplastic polyurethane. J Cell Plas 2017;53:373-388. doi.org/10.1177/0021955X16652107.
[90] Jayavardhan ML, Bharath Kumar BR, Doddamani M, Singh AK, Zeltmann SE, Gupta N. Development of glass microballoon/HDPE syntactic foams by compression molding. Compos. B. Eng. 2017;130:119-131. doi.org/10.1016/j.compositesb.2017.07.037.
[91] Jayavardhan ML, Doddamani M. Quasi-static compressive response of compression molded glass microballoon/HDPE syntactic foam. Compos. B. Eng. 2018;149:165-177. doi.org/10.1016/j.compositesb.2018.04.039
[92] Singh AK, Deptula AJ, Anawal R, Doddamani M, Gupta N. Additive manufacturing of three-phase syntactic foams containing glass microballoons and air pores. JOM 2019;7:1520-1527. doi.org/10.1007/s11837-019-03355-5.
[93] Singh A, Saltonstall B, Patil B, Hoffmann N, Doddamani M, Gupta N. Additive Manufacturing of Syntactic Foams: Part 2: Specimen Printing and Mechanical Property Characterization. JOM. 2018;70:310-314. doi.org/10.1007/s11837-017-2731-x.
[94] Bonthu D, Bharath HS, Gururaja S, Prabhakar P, Doddamani M. 3D printing of syntactic foam cored sandwich composite. JCOMC. 2020;3:100068. doi.org/10.1016/j.jcomc.2020.100068
[95] Bharath HS, Bonthu D, Gururaja S, Prabhakar P, Doddamani M. Flexural response of 3D printed sandwich composite. Compos Struct 2021;263:113732. doi.org/10.1016/j.compstruct.2021.113732.
[96] Nawafleh N, Wright W, Dariavach N, Celik E. 3D-printed thermoset syntactic foams with tailorable mechanical performance. J Mater Sci 2020;55:16048-16057. doi.org/10.1007/s10853-020-05111-6.
[97] Bharath HS, Bonthu D, Prabhakar P, Doddamani M. Three-Dimensional Printed Lightweight Composite Foams. ACS Omega. 2020;5:22536-22550. doi.org/10.1021/acsomega.0c03174.
[98] Sorrentino L, Aurilia M, Forte G, Iannace S. Anisotropic Mechanical Behavior of Magnetically Oriented Iron Particle Reinforced Foams. J Appl Polym Sci 2011;119:1239-1247. doi.org/10.1002/app.32603.
[99] Li YP, Qi S, Fu J, Gan RY, Yu M. Fabrication and mechanical behaviors of iron-

nickel foam reinforced magnetorheological elastomer. Smart Mater Struct. 2019;28:115039. doi.org/10.1088/1361-665X/ab49de.
[100] Zhao JC, Zhao QL, Wang GL, Wang CD, Park CB. Injection Molded Strong Polypropylene Composite Foam Reinforced with Rubber and Talc. Macromol Mater Eng. 2020;305:1900630. doi.org/10.1002/mame.201900630.
[101] Maharsia R, Gupta N, Jerro HD. Investigation of flexural strength properties of rubber and nanoclay reinforced hybrid syntactic foams.Mater Sci Eng A 2006;417:249-258. doi.org/10.1016/j.msea.2005.10.063.
[102] Lebar A, Oddy A, Aguiar R, Petel OE. Effect of Interface Adhesion on the Spall Strength of Particle-Reinforced Polymer Matrix Composites. SCCM 2020;2272:120012. doi.org/10.1063/12.0000781.
[103] Huang W, Xu HJ, Fan ZH, Ao YL, Liu JY. Compressive response of composite ceramic particle-reinforced polyurethane foam. Polym Test. 2020;87:106514. doi.org/10.1016/j.polymertesting.2020.106514.
[104] Yang ZG, Zhao B, Qin SL, Hu ZF, Jin ZK, Wang JH. Study on the mechanical properties of hybrid reinforced rigid polyurethane composite foam. J Appl Polym Sci 2004;92:1493-1500. doi.org/10.1002/app.20071.
[105] Brown KA, Brooks R, Awoyemi, O. Meso-scale modelling of shock wave propagation in a cellular glass particle reinforced thermoplastic composite. In: 18th International Conference of Composites Materials (ICCM18).
[106] Cao SZ, Lu Y, Ma N, Yang T, Zhang YW. Reinforcement mechanisms of recycled glass beads reinforced thermoplastic foams under dynamic compressions. Constr Build Mater 2022;344:128094. doi.org/10.1016/j.conbuildmat.2022.128094.
[107] Kumar BRB, Singh AK, Doddamani M, Luong DD, Gupta N. Quasi-Static and High Strain Rate Compressive Response of Injection-Molded Cenosphere/HDPE Syntactic Foam. JOM. 2016;68:1861-1871. doi.org/10.1007/s11837-016-1912-3.
[108] Yousaf Z, Morrison NF, Parnell WJ. Tensile properties of all-polymeric syntactic foam composites: Experimental characterization and mathematical modelling. Compos B Eng 2022;231:109556. doi.org/10.1016/j.compositesb.2021.109556.
[109] Curd ME, Morrison NF, Smith MJA, Gajjar P, Yousaf Z, Parnell WJ. Geometrical and mechanical characterisation of hollow thermoplastic microspheres for syntactic foam applications. Compos B Eng 2021;223,108952. doi.org/10.1016/j.compositesb.2021.108952.
[110] Wang M, Xu S. Preparation and Applications of Foam Ceramics. IOP Conf Ser Earth Environ Sci 2018;186:012066. doi :10.1088/1755-1315/186/2/012066.
[111] Sedlacik M, Nguyen M, Opravil T, Sokolar R. Preparation and Characterization of Glass-Ceramic Foam from Clay-Rich Waste Diatomaceous Earth. Mater. 2022;15:1384. doi: 10.3390/ma15041384
[112] Bai F. One dimensional thermal analysis of silicon carbide ceramic foam used for solar air receiver. Int J Therm Sci 2010;49:2400-2904. doi.org/10.1016/j.ijthermalsci.2010.08.010.
[113] Betke U, Scheunemann M, Scheffler M. Refitting of Zirconia Toughening into Open-Cellular Alumina Foams by Infiltration with Zirconyl Nitrate. Mater. 2019;12:1886. doi: 10.3390/ma12121886.

[114] Sarkar N, Park JG, Mazumder S, Pokhrel A, Aneziris CG, Kim IJ. Effect of amphiphile chain length on wet foam stability of porous ceramics. Ceram Int 2015;41:4021-4027. /doi.org/10.1016/j.ceramint.2014.11.089.
[115] Sarkar N, Park JG, Mazumder S, Aneziris CG, Kim IJ. Processing of particle stabilized Al2TiO5-ZrTiO4 foam to porous ceramics. J Eur Ceram Soc 2015;35:3969-76. doi.org/10.1016/j.jeurceramsoc.2015.07.004.
[116] Byun YM, Lee GW, Lee KS, Park JG, Kim IJ. Mechanical properties of carbon fiber-reinforced Al2O3 porous ceramics. J Korean Ceram Soc 2021;58:269-275. doi.org/10.1007/s43207-020-00105-1.
[117] Pokhrel A, Seo DM, Lee ST, Kim IJ. Processing of Porous Ceramics by Direct Foaming: A Review. J Korean Ceram Soc 2013;50:93-102. doi.org/10.4191/kcers.2013.50.2.093.
[118] Yu J, Yang J, Li H, Xi X, Huang Y. Study on particle-stabilized Si3N4 ceramic foams. Mater Lett 2011;65:1801-1804. doi.org/10.1016/j.matlet.2011.03.082.
[119] Zhang M, Li X, Zhang M, Xiu Z, Li J-G, Li J, et al. High-strength macro-porous alumina ceramics with regularly arranged pores produced by gel-casting and sacrificial template methods. J Mater Sci 2019;54:10119-10129. doi.org/10.1007/s10853-019-03576-8.
[120] Ozcivici E, Singh RP. Fabrication and characterization of ceramic foams based on silicon carbide matrix and hollow alumino-silicate spheres. J Am Ceram Soc 2005;88:3338-3345. doi.org/10.1111/j.1551-2916.2005.00612.x.
[121] Kim IJ, Park JG, Han YH, Kim SY, Shackelford JF. Wet Foam Stability from Colloidal Suspension to Porous Ceramics: A Review. J Korean Ceram Soc 2019;56:211-232. doi.org/10.4191/kcers.2019.56.3.02
[122] Zheng Y, Luo X, You J, Peng Z, Zhang S. Ceramic foams with highly open channel structure from direct foaming method in combination with hollow spheres as pore-former. J Asian Ceram Soc. 2021;9:24-29. /doi.org/10.1080/21870764.2020.1847427.
[123] Fey T, Betke U, Rannabauer S, Scheffler M. Reticulated Replica Ceramic Foams: Processing, Functionalization, and Characterization. Adv Eng Mater. 2017;19:1700369. doi.org/10.1002/adem.201700369.
[124] Voigt C, Aneziris CG, Hubalkova J. Rheological Characterization of Slurries for the Preparation of Alumina Foams via Replica Technique. J Am Ceram Soc 2015;98:1460-1463. doi.org/10.1111/jace.13522.
[125] Zhang YH. Microstructures and mechanical properties of silicon nitride bonded silicon carbide ceramic foams. Mater Res Bull 2004;39:755-761. doi.org/10.1016/j.materresbull.2004.02.004.
[126] Pokhrel A, Park JG, Nam JS, Cheong DS, Kim IJ. Stabilization of Wet Foams for Porous Ceramics Using Amphiphilic Particles. J Korean Ceram Soc 2011;48:463-466 doi.org/10.4191/kcers.2011.48.5.463..
[127] Liu J, Ren B, Rong Y, Zhao Y, Wang L, Lu Y, et al. Highly porous alumina cellular ceramics bonded by in-situ formed mullite prepared by gelation-assisted Al2O3-Si particle-stabilized foams. Ceram Int 2020;46:12282-12287. doi.org/10.1016/j.ceramint.2020.01.278.

[128] Huo W-L, Zhang X-Y, Chen Y-G, Lu Y-J, Liu W-T, Xi X-Q, et al. Highly Porous Zirconia Ceramic Foams with Low Thermal Conductivity from Particle-Stabilized Foams. J Am Ceram Soc 2016;99:3512-3515. doi.org/10.1111/jace.14555.
[129] Geng H, Liu J, Guo A, Ren S, Xu X, Liu S. Fabrication of heat-resistant syntactic foams through binding hollow glass microspheres with phosphate adhesive. Mater Des. 2016;95:32-38. doi.org/10.1016/j.matdes.2016.01.108.
[130] Liu J, Li X, Zhou C. Mechanical and thermal properties of modified red mud-reinforced phenolic foams. Polym Int 2018;67:528-534. https://doi.org/10.1002/pi.5540.
[131] Huang C, Huang Z, Wang Q. Effect of high-temperature treatment on the mechanical and thermal properties of phenolic syntactic foams. Polym Eng Sci. 2018;58:2200-2209. doi.org/10.1002/pen.24835.
[132] Qiu C, Li F, Wang L, Zhang X, Zhang Y, Tang Q, et al. The preparation and properties of polyurethane foams reinforced with bamboo fiber sources in China. Mater Res Express. 2021;8:045501. doi.org/10.1088/2053-1591/abf1cd.
[133] John B, Nair CPR, Ninan KN. Effect of nanoclay on the mechanical, dynamic mechanical and thermal properties of cyanate ester syntactic foams. Mater Sci Eng A 2010;527:5435-5443. doi.org/10.1016/j.msea.2010.05.016.
[134] Song SA, Lee Y, Kim YS, Kim SS. Mechanical and thermal properties of carbon foam derived from phenolic foam reinforced with composite particles. Compos Struct 2017;173:1-8. doi.org/10.1016/j.compstruct.2017.04.001
[135] Wu B, Chen R, Fu R, Agathopoulos S, Su X, Liu H. Low thermal expansion coefficient and high thermal conductivity epoxy/Al2O3/T-ZnOw composites with dual-scale interpenetrating network structure. Compos Part A Appl Sci. 2020;137:105993. doi.org/10.1016/j.compositesa.2020.105993.
[136] Wang H, Li L, Wei X, Hou X, Li M, Wu X, et al. Combining Alumina Particles with Three-Dimensional Alumina Foam for High Thermally Conductive Epoxy Composites. ACS Appl Polym Mater 2021;3:216-25. doi.org/10.1021/acsapm.0c01055.
[137] Zhao LZ, Zhao MJ, Cao XM, Tian C, Hu WP, Zhang JS. Thermal expansion of a novel hybrid SiC foam-SiC particles-Al composites. Compos Sci Technol. 2007;67:3404-3408. doi.org/10.1016/j.compscitech.2007.03.020.
[138] Chen SM, Jiang Y. The acoustic property study of polyurethane foam with addition of bamboo leaves particles. Polym Compos 2018;39:1370-1381. doi.org/10.1002/pc.24078.
[139] Tiuc AE, Nemes O, Vermesan H, Toma AC. New sound absorbent composite materials based on sawdust and polyurethane foam. Compos B Eng 2019;165:120-30. doi.org/10.1016/j.compositesb.2018.11.103.
[140] Zangiabadi Z, Hadianfard MJ. The role of hollow silica nanospheres and rigid silica nanoparticles on acoustic wave absorption of flexible polyurethane foam nanocomposites. J Cell Plast 2020;56:395-410. doi.org/10.1177/0021955X19864388.
[141] Muhazeli NS, Nordin NA, Ubaidillah U, Mazlan SA, Aziz SAA, Nazmi N, et al. Magnetic and Tunable Sound Absorption Properties of an In-Situ Prepared Magnetorheological Foam. Mater 2020;13:5637. doi.org/10.3390/ma13245637.

[142] Oh JH, Kim JS, Nguyen VH, Oh IK. Auxetic graphene oxide-porous foam for acoustic wave and shock energy dissipation. Compos B Eng 2020;186:107817. doi.org/10.1016/j.compositesb.2020.107817.
[143] Zhang CH, Li JQ, Hu Z, Zhu FL, Huang YD. Correlation between the acoustic and porous cell morphology of polyurethane foam: Effect of interconnected porosity. Mater Des 2012;41:319-325. doi.org/10.1016/j.matdes.2012.04.031.
[144] Liu Y, Guan Y, Li Y, Zhai J, Li X, Lin J. Rheological/crystallization behavior of PP/graphite nanosheet composites and performance of microcellular foaming plastics. Compos Commun. 2022;32:101133. doi.org/10.1016/j.coco.2022.101133.
[145] Liu H, Zhang F, Li H, Xiw H, Jiang C, Xie L. Modified holow glass microsphere isocyanate-based polyimide foam composite with improved mechanical and thermal insulation properties. High Perform Polym. 2022;34:465-473. doi.org/10.1177/09540083221074606.
[146] Cosse RL, Araujo FH, Pinto FANC, de Carvalho LH, de Morais ACL, Barbosa R, et al. Effects of the type of processing on thermal, morphological and acoustic properties of syntactic foams. Compos B Eng. 2019;173:106933. doi.org/10.1016/j.compositesb.2019.106933.
[147] Raut SV, Kanthale VS, Kothavale VS. Review on application of aluminum foam in sound absorption technology. Int. J. Curr. Eng. Tech. 2016;3:178-181. DOI:10.14741/Ijcet/22774106/spl.4.2016.36.
[148] Wu J, Li C, Wang D, Gui M. Damping and sound absorption properties of particle reinforced AI matrix composite foams. Compos. Sci. Technol. 2003;63:569-574. DOI:10.1016/S0266-3538(02)00215-4.
[149] Sandhya, P.K., Sreekala, M.S., Thomas, S. (2022). Phenolic-Based Foams: State of the Art, New Challenges, and Opportunities. In: P.K, S., M.S., S., Thomas, S. (eds) Phenolic Based Foams. Gels Horizons: From Science to Smart Materials. Springer, Singapore. https://doi.org/10.1007/978-981-16-5237-0_1.
[150] Gupta N, Priya S, Islam R, Ricci W. Characterization of mechanical and electrical properties of epoxy-glass microballoon syntactic composites. Ferroelectrics 2006;345:1-12. doi.org/10.1080/00150190601018002.
[151] Shunmugasamy VC, Pinisetty D, Gupta N. Electrical properties of hollow glass particle filled vinyl ester matrix syntactic foams. J Mater Sci 2014;49:180-190. doi.org/10.1007/s10853-013-7691-0.
[152] Poveda RL, Gupta N. Electrical properties of carbon nanofiber reinforced multiscale polymer composites. Mater Des 2014;56:416-422. doi.org/10.1016/j.matdes.2013.11.074.
[153] Abedin R, Feng X, Pojman J, Ibekwe S, Mensah P, Warner I, et al. A Thermoset Shape Memory Polymer-Based Syntactic Foam with Flame Retardancy and 3D Printability. ACS Appl Polym Mater 2022;4:1183-1195. doi.org/10.1021/acsapm.1c01596.
[154] Ge Z, Chen H, Ren Y, Xiao P, Yang Y, Zhang T, et al. A Universal Method for the Preparation of Dual Network Reduced Graphene Oxide-Ceramic/Metal Foam Materials with Tunable Porosity and Improved Conductivity. Chem Mater 2018;30:8368-8374. doi.org/10.1021/acs.chemmater.8b04081.

[155] Chen Y, Zhang X, Wu Z, Li F, Gan X, Tao J, et al. Silver composites with an inhomogeneous structure reinforced by CNTs/Cu composite foams as 3-dimentional skeleton. Mater Today Commun 2022;30:103022. doi.org/10.1016/j.mtcomm.2021.103022.
[156] Peng Y, Liu H, Li T, Zhang J. Hybrid Metallic Foam with Superior Elasticity, High Electrical Conductivity, and Pressure Sensitivity. ACS Appl Mater Interface 2020;12:6489-495. doi.org/10.1021/acsami.9b20652.
[157] Cao SZ, Liu T. Self-healing Synthetic Epoxy Foam under Cyclic Quasi-Static Compressive Loading. Sampe J 2021;57:38-44.
[158] McGugan M, Pereira G, Sorensen BF, Toftegaard H, Branner K. Damage tolerance and structural monitoring for wind turbine blades. Philos Tran Royal Soc A 2015;373:20140077. doi.org/10.1098/rsta.2014.0077.
[159] Cao SZ, Liu T. Compressive response of self-healing polymer foams containing bilayered capsules: Coupled healing agents diffusion and stress simulations. J Mech Phys Solids 2021;149:104314. doi.org/10.1016/j.jmps.2021.104314.
[160] John B, Reghunadhan Nair CP. Thermosetting polymer based syntactic foams: an overview. Handbook of Thermoset Plastics(Fourth Edition). 2022;801-832. doi.org/10.1016/B978-0-12-821632-3.00020-8
[161] Wang Y, Bolanos E, Wudl F, Hahn T, Kwok N. Self-healing polymers and composites based on thermal activation. Proc SPIE. 6526, Behavior and Mechanics of Multifunctional and Composite Materials 2007:65261. doi.org/10.1117/12.715507.
[162] Zhan YH, Cheng Y, Yan N, Li YC, Meng YY, Zhang CM, et al. Lightweight and self-healing carbon nanotube/acrylic copolymer foams: Toward the simultaneous enhancement of electromagnetic interference shielding and thermal insulation. Chem Eng J 2021;417:129339. doi.org/10.1016/j.cej.2021.129339
[163] Quadrini F, Bellisario D, Iorio L, Santo L, Pappas P, Koutroumanis N, et al. Shape Memory Composite Sandwich Structures with Self-Healing Properties. Polymers. 2021;13:3056. doi.org/10.3390/polym13183056.
[164] Singh AK, Shishkin A, Koppel T, Gupta N. A review of porous lightweight composite materials for electromagnetic interference shielding. Compos. B. Eng. 2018;149:188-197. doi.org/10.1016/j.compositesb.2018.05.027.
[165] Gupta N, Zeltmann SE, Shummugassamy VC, Pinisetty D. Applications of polymer matrix syntactic foams. JOM 2014;66:245-254. DOI: 10.1007/s11837-013-0796-8.
[166] Zhang L, Roy S, Chen Y, Chua EK, See KY, Hu X, Liu M. Mussel-inspired polydopamine coated hollow carbon microspheres, a novel versatile filler for fabrication of high performance syntactic foams. ACS Appl. Mater. Interfaces 2014;6:18644-18652. doi.org/10.1021/am503774a
[167] Panigrahi R, Srivastave SK, Trapping of microwave radiation in hollow polypyrrole microsphere through enhanced internal reflection: A novel approach. Sci. Rep. 2015;5:7638. DOI: 10.1038/srep07638.
[168] Yu X, Shen Z. The electromagnetic shielding of Ni films deposited on cenosphere particles by magnetron sputtering method. J. Magn. Magn, Mater. 2009;321:2890-2895. doi.org/10.1016/j.jmmm.2009.04.040.

[169] Yao F, Xie W, Ma Chao, Wang D, EI-Bahy ZM, Helal MH, Liu H, Guo Z, Gu H. Superb electromagnetic shielding polymer nanocomposites filled with 3-dimensional p-phenylenediamine/aniline copolymer nanofibers@copper foam hybrid nanofillers. Compos B Eng 2022;110236. doi.org/10.1016/j.compositesb.2022.110236.
[170] Li S, Guo X, Liao J, Li Q, Sun G. Crushing analysis and design optimization for foam-filled aluminum/CFRP hybrid tube against transverse impact. Compos. B. Eng. 2020;196:108029. doi.org/10.1016/j.compositesb.2020.108029.
[171] Ahmadi H, Liaghat G, Charandabi SC. High velocity impact on composite sandwich panels with nano-reinforced syntactic foam core. Thin-walled Struct. 2020;148:106599. https://doi.org/10.1016/j.tws.2019.106599
[172] Huang W, Xu H, Fan Z, Jiang W, Liu J. Dynamic failure of ceramic particle reinforced foam-filled composite lattice core. Compos. Sci. Technol. 2020;193:108143. /doi.org/10.1016/j.compscitech.2020.108143
[173] Pareta AS, Gupta R, Panda SK. Experimental investigation on fly ash particulate reinforcement for property enhancement of PU foam core FRP sandwich composites. Compos. Sci. Technol. 2020;195:108207. doi.org/10.1016/j.compscitech.2020.108207.
[174] Wang L, Zhang B, Zhang J, Jiang Y, Wang W, Wu G. Deformation and energy absorption properties of cenosphere-aluminum syntactic foam-filled tubes under axial compression. Thin-walled Struct. 2021;160:107364. doi.org/10.1016/j.tws.2020.107364.
[175] Zhang B, Wang L, Zhang J, Jiang Y, Wu G. Deformation and energy absorption properties of cenosphere/aluminum syntactic foam-filled circular tubes under lateral quasi-static compression. Int. J. Mech. Sci. 2021;192:106126. doi.org/10.1016/j.ijmecsci.2020.106126.
[176] Thiyagarajan R, Senthil Kumar M. A review on closed cell metal matrix syntactic foams: a green initiative towards eco-sustainability. Mater. Manu. Process. 2021; 36:1333-1351. doi.org/10.1080/10426914.2021.1928696.
[177] Sun G, Guo X, Li S, Ruan D, Li Q. Comparative study on aluminum/GFRP/CFRP tubes for oblique lateral crushing. Thin-walled Struct. 2020;152:106420. doi.org/10.1016/j.tws.2019.106420.
[178] Qi Z, Zhang Y, Lin Y, Lu F, Chen R. Dynamic embedding behavior of thin-wall expansion tube loaded by explosive shock wave. Int. J. Impact Eng. 2022;168:104290. doi.org/10.1016/j.ijimpeng.2022.104290
[179] Li S, Guo X, Liao J, Li Q, Sun G. Crushing analysis and design optimization for foam-filled aluminum/CFRP hybrid tube against transverse impact. Compos. B. Eng. 2020;196:108029.
[180] Thiyagarajan R, Kumar MS. A Review on Closed Cell Metal Matrix Syntactic Foams: A Green Initiative towards Eco-Sustainability. Mater Manuf Process 2021;36:1333-1351. doi.org/10.1080/10426914.2021.1928696.
[181] Wang P, Zhong S, Yan K, Liao B, Zhang J. Influence of a batch of hollow glass microspheres with different strength grades on the compression strength of syntactic foam. Compos Sci Technol 2022;223:109442. doi.org/10.1016/j.compscitech.2022.109442.
[182] Sarrafan S, Feng X, Li G. A soft syntactic foam actuator with high recovery stress,

actuation strain, and energy output. Mater Today Commun 2022;31:103303. doi.org/10.1016/j.mtcomm.2022.103303.
[183] D'Auria M, Davino D, Pantani R, Sorrentino L. Magnetic field-structuring as versatile approach to shape the anisotropic mechanical response of composite foams. Compos B Eng 2021;212:108659. doi.org/10.1016/j.compositesb.2021.108659.
[184] Auria MD, Davino D, Pantani R, Sorrentino L. Magnetic field-structuring as versatile approach to shape the anisotropic mechanical response of composite foam. Compos B Eng 2021; 212:108659. doi.org/10.1016/j.compositesb.2021.108659.
[185] Anirudh S, Jayalakshmi CG, Anand A, Kandasubramanian B, Ismail SO. Epoxy/hollow glass microsphere syntactic foams for structural and functional application-A review. Eur Polym J. 2022;171:111163. doi.org/10.1016/j.eurpolymj.2022.111163.
[186] Shishkin A, Hussainova I, Kozlov V, Lisnanskis M, Leroy P, Lehmhus D. Metal-Coated Cenospheres Obtained via Magnetron Sputter Coating: A New Precursor for Syntactic Foams. JOM. 2018;70:1319-1325. doi.org/10.1007/s11837-018-2886-0.
[187] Hasanzadeh R, Azdast T, Mojaver M, Darvishi MM, Park CB. Cost-effective and reproducible technologies for fabrication of tissue engineered scaffolds: The state-of-the-art and future perspectives. Polym. 2022;244:124681. doi.org/10.1016/j.polymer.2022.124681.
[188] Liu C, Le L, Zhang M, Ding J. Tunable Large-Scale Compressive Strain Sensor Based on Carbon Nanotube/Polydimethylsiloxane Foam Composites by Additive Manufacturing. Adv Eng Mater 2021;2101337 doi.org/10.1002/adem.202101337.
[189] Orbulov IN, Szlancsik A, Kemeny A, Kincses D. Low-Cost Light-Weight Composite Metal Foams for Transportation Applications. J Mater Eng Perform 2022 doi.org/10.1007/s11665-022-06644-4.
[190] Han SK, Song M, Choi K, Choi SW. Fabrication of Biodegradable Polyurethane Foam Scaffolds with Customized Shapes and Controlled Mechanical Properties by Gas Foaming Technique. Macromol Mater Eng 2021;306:2100114. doi.org/10.1002/mame.202100114.
[191] Bharath HS, Sawardekar A, Wadder S, Jeyaraj P, Doddamani M. Mechanical behavior of 3D printed syntactic foam composites. Compos Struct 2020; 254:112832. doi.org/10.1016/j.compstruct.2020.112832.
[192] Bharath HS, Wadder S, Bekinal SI, Jeyaraj P, Doddamani M. Effect of axial compression on dynamic response of concurrently printed sandwich. Compos Struct 2021; 259: 113223. doi.org/10.1016/j.compstruct.2020.113223
[193] Dileep B, Prakash R, Bharath HS, Jeyaraj P, Doddamani M. Dynamic behavior of concurrently printed functionally graded closed-cell foams. Compos Struct 2021; 275:114449. doi.org/10.1016/j.compstruct.2021.114449.
[194] Reichler M, Rabensteiner S, Tornblom L, Coffeng S, Viitanen L, Jannuzzi L. Scalable method for bio-based solid foams that mimic wood. Sci Rep. 2021;11:24306. doi.org/10.1038/s41598-021-03764-0.
[195] Qu HW, Fu HY, Han ZY, Sun Y. Biomaterials for bone tissue engineering scaffolds: a review. RSC Adv 2019;9:26252. doi.org/10.1039/C9RA05214C.
[196] Greer JR, Deshpande VS. Three-dimensional architected materials and structures:

Design, fabrication, and mechanical behavior. MRS Bull 2019;44:750-757. doi.org/10.1557/mrs.2019.232.
[197] Shercliff HR, Ashby MF. Elastic Structures in Design. Reference Module in Materials Science and Materials Engineering: Elsevier; 2016. doi.org/10.1016/B978-0-12-803581-8.02944-1.
[198] Zhang YW, Liu T, Tizani W. Experimental and numerical analysis of dynamic compressive response of Nomex honeycombs. Compos B Eng 2018;148:27-39. doi.org/10.1016/j.compositesb.2018.04.025.
[199] Wang L, Zhang B, Zhang J, Jiang Y, Wang W, Wu, G. Deformation and energy absorption properties of cenosphere-aluminum syntactic foam-filled tubes under axial compression. Thin Wall Struct 2021; 160:107364. https://doi.org/10.1016/j.tws.2020.107364.
[200] Jin Q, Wang J, Chen J, Bao F. Axial compressive behavior and energy absorption of syntactic foam-filled GFRP tubes with lattice frame reinforcement. Compos Struct 2022; 299:116080. doi.org/10.1016/j.compstruct.2022.116080.
[201] Pagliocca N, Youssef G, Koohbor B. In-Plane mechanical and failure responses of honeycombs with syntactic foam cell walls. Compos Struct 2022; 295:115866. doi.org/10.1016/j.compstruct.2022.115866.
[202] Cheneler D, Kennedy R. Measurement and modelling of the elastic defection of novel metal syntactic foam composite sandwich structures in 3-point bending. Compos Struct 2020; 235: 111817. doi.org/10.1016/j.compstruct.2019.111817.
[203] Chen J, Zhang P, Cheng Y, Liu J. On the crushing response of the functionally graded metallic foams based on 3D Voronoi model. Thin Wall Struct 2020; 157:107085. https://doi.org/10.1016/j.tws.2020.107085.
[204] Zheng G, Zhang L, Wang E, Yao R, Luo Q, Li Q, Sun G. Investigation into multiaxial mechanical behaviors of Kelvin and Octet - B polymeric closed-cell foams. Thin Wall Struct 2022; 177:109405. https://doi.org/10.1016/j.tws.2022.109405.
[205] Zhang H, Chang B, Peng K, Yu J, Zhang Z. Anti-blast analysis and design of a sacrificial cladding with graded foam-filled tubes. Thin Wall Struct 2023; 182 Part B:110313. https://doi.org/10.1016/j.tws.2022.110313.
[206] Bauer J, Hengsbach S, Tesari I, Schwaiger R, Kraft O. High-strength cellular ceramic composites with 3D microarchitecture. Proc Natl Acad Sci USA. 2014;111:2453-2458. doi.org/10.1073/pnas.131514711.
[207] Gahlen P, Stommel M. Modeling of the local anisotropic mechanical foam properties in polyisocyanurate metal panels using mesoscale FEM simulations. Int J Solids Struct 2022;244-245. doi.org/10.1016/j.ijsolstr.2022.111595.
[208] Campillo M, Sedaghati R, Drew RAL, Alfonso I, Perez L. Development of an RVE using a DEM-FEM scheme under modified approximate periodic boundary condition to estimate the elastic mechanical properties of open foams. Eng Comput 2021. doi.org/10.1007/s00366-021-01355-1.
[209] Yang H, Abali BE, Müller WH, Barboura S, Li J. Verification of asymptotic homogenization method developed for periodic architected materials in strain gradient continuum. Int J Solids Struct 2022;238:111368. doi.org/10.1016/j.ijsolstr.2021.111386.
[210] Liang H, Niazi Angili S, Morovvati M, Li X, Saber-Samandari S, Yusof MYPM,

et al. Fabrication and characterization of wollastonite-titanium porous scaffold for pharmaceutical application: Representative volume element simulation. Mater Sci Eng B 2022;280:115684. doi.org/10.1016/j.mseb.2022.115684.
[211] Kaya AC, Zaslansky P, Fleck C. Modeling of Complex Gray Cast Iron Open‐Cell Foams Revealing Insights on Failure and Deformation on Different Hierarchical Length‐Scales. Adv Eng Mater 2021;24:2100677. doi.org/10.1002/adem.202100677.
[212] Bensalem I, Benhizia A. Novel design of irregular closed-cell foams structures based on spherical particle inflation and evaluation of its compressive performance. Thin Wall Struct 2022; 181:109991. https://doi.org/10.1016/j.tws.2022.109991.
[213] Cao SZ, Zhang YW, Lu Y. Mechanical properties and reinforcement mechanisms evaluation of closed-cell polymer foams reinforced by recycled glass beads. Constr Build Mater 2021;275:122062. doi.org/10.1016/j.conbuildmat.2020.122062.
[214] Carolan D, Mayall A, Dear JP, Fergusson AD. Micromechanical modelling of syntactic foam. Compos B Eng. 2020; 183:107701. doi.org/10.1016/j.compositesb.2019.107701.
[215] Prabhakar P, Feng H, Subramaniyan SP, Doddamani M. Densification mechanics of polymeric syntactic foams. Compos B Eng. 2022; 232:109597. doi.org/10.1016/j.compositesb.2021.109597.
[216] Thiyagarajan R, Senthil Kumar M. A Review on Closed Cell Metal Matrix Syntactic Foams: A Green Initiative towards Eco-Sustainability. Mater Manu Process 2021;36:1333-1351. doi.org/10.1080/10426914.2021.1928696.
[217] Pietras D, Linul E, Sadowski T, Rusinek A, Out-of-plane crushing response of aluminum honeycombs in-situ filled with graphene-reinforced polyurethane foam. Compos Struct 2020; 249:112548. doi.org/10.1016/j.compstruct.2020.112548.
[218] Zhang L, Townsend D, Petrinic N, Pellegrino A. The dependency of compressive response of epoxy syntactic foam on the strain rate and temperature under rigid confinement. Compos Struct 2022; 280:114853. doi.org/10.1016/j.compstruct.2021.114853.
[219] Yu T, Jiang F, Wang J, Wang Z, Chang Y, Guo C. Acoustic insulation and absorption mechanism of metallic hollow spheres composites with different polymer matrix. Compos Struct 2020; 248:112566. doi.org/10.1016/j.compstruct.2020.112566.
[220] Choi WH, Kwak BS, Kweon JH, Nam YW. Radar-absorbing foam-based sandwich composite with electroless nickel-plated glass fabric. Compos Struct. 2020; 243:112252. doi.org/10.1016/j.compstruct.2020.112252.
[221] Brooks AL, Shen ZL, Zhou HY. Development of a high-temperature inorganic synthetic foam with recycled fly-ash cenospheres for thermal insulation brick manufacturing. J Clean Prod 2020;246:118748. doi.org/10.1016/j.jclepro.2019.118748.
[222] Schmid ED, Veluswamy NKP, Salem DR. Mechanical and thermal properties of microchannel insulating foams comprising a multifunctional epoxy/polyhedral oligomeric silsesquioxane nanocomposite. Polym Compos 2020;41:5030-5042. doi.org/10.1002/pc.25772.
[223] Chen YX, Klima KM, Brouwers HJH, Yu Q. Effect of silica aerogel on thermal insulation and acoustic absorption of geopolymer foam composites: The rile of aerogel particle size. Compos B Eng 2022;242:110048.

doi.org/10.1016/j.compositesb.2022.110048.
[224] Lin B, Yuen ACY, Oliver S, Liu J, Yu B, Yang W, Wu S, Yeoh GH, Wang CH. Dual functionalisation of polyurethane foam for unprecedented flame retardancy and antibacterial properties using layer-by-layer assembly of MXene chitosan with antibacterial metal particles. Compos B Eng 2022;244:110147. doi.org/10.1016/j.compositesb.2022.110147.
[225] Sun L, Cai Y, Haider MK, Miyagi D, Zhu C, Kim LS. Structural design and optimization of metal-organic framework-derived FeOx@/rGO anode materials for constructing high-performance hybrid supercapacitors. 2022; 236:109812. doi.org/10.1016/j.compositesb.2022.109812.